Wave orbital motion on the Dutch lower shoreface: observations, parameterizations and effects on bed-load sediment transport

Bachelor Thesis

10-07-2018

B.A. Treurniet
s1539159

Bachelor Civil Engineering – University of Twente
Water Engineering & Management Department

University of Twente supervisor:	Ir. H. (Harriëtte) Holzhauer
Rijkswaterstaat supervisor:	Ir. R.J.A. (Rinse) Wilmink
Deltares supervisor:	Dr. Ir. B.T. (Bart) Grasmeijer

UNIVERSITEIT TWENTE.

Rijkswaterstaat
Ministerie van Infrastructuur en Waterstaat

Deltares

1. Preface

This thesis report is written as final part of the bachelor Civil Engineering of the University of Twente. The study concerns an investigation into orbital wave motion on the Dutch lower shoreface and effects of orbital wave motion on bed-load sediment transport. The research is conducted in collaboration with Rijkswaterstaat and Deltares, where I worked within unit Water, Transport and Living Environment, department highwater safety and unit coastal engineering, department morphology respectively.

I would like to thank my supervisors from Rijkswaterstaat and Deltares, Ir. R.J.A. Wilmink and Dr. Ir. B.T. Grasmeijer for the effort they made in helping me during my research. Their eagerness to know the results of the data-analysis worked contagious. I would like to thank them for their useful advices and insights on coastal management and morphodynamical processes on the Dutch shoreface, as well on doing research at a whole. I also like to thank Ir. H. Holzhauer, for her honest remarks and sharp advices, which kept me focussed. At last, I would like to thank my colleagues at Rijkswaterstaat, who made me feel welcome in their midst.

Enjoy reading this Bachelor thesis report,

Bart Treurniet,

Enschede, 10-07-2018

2. Abstract

As part of the Coastal Genesis 2.0 campaign, orbital wave velocities are measured with Acoustic Doppler Velocimeters at two different locations on the lower shoreface near the Amelander Zeegat, at -16m and -20m NAP. Using the Van Rijn (2007) sediment transport formulations, year-round weighted averaged bed-load sediment transports due to wave orbital motion of 11,5 $m^3/y/m$ and 3,2 $m^3/y/m$ are found for -16m and -20m NAP respectively in a direction almost in line with the wave direction.

Parameterizations by Isobe & Horikawa (1982) and Ruessink et al. (2012) predict a near-bed wave velocity profile as a function of surface wave characteristics. The velocity profile is compared with the orbital wave velocities, measured with the ADV's. The Isobe&Horikawa parameterization shows more skewed waves than the Ruessink parameterization, but lower significant orbital velocities. Orbital wave velocities have a larger influence on bed-load sediment transport than skewness. Bed-load sediment transports calculated with the Isobe & Horikawa parameterization approximates the bed-load sediment transport rates, calculated from measured orbital velocities best.

The found sediment transport rates at -20m could be used to make an estimation about net-sediment transport into the coastal foundation. The -20m NAP contour is the seaward border of the coastal foundation, which must be maintained by sand nourishments. In the 3rd Coastal Memorandum (3e Kustnota) is decided that yearly 12Mm^3 sand should be nourished to the coastal foundation, assuming negligible sediment transport takes place over the -20m NAP contour. The found bed-load sediment transport rate at -20m NAP of 3,5 $m^3/y/m$ comes down to nearly 1 Mm^3 per year. Extrapolated to the entire Dutch shoreline, this is a considerable amount.

Table of contents

3. Introduction

This thesis contains the report of the bachelor thesis research into wave orbital motion on the Dutch lower shoreface. In this introduction, the research context and research aim and questions are discussed. Then the background information for this research is described. The background information chapter is extensive, because of the high level of detail of this bachelor thesis. A description of the available data is presented, followed by the research methods used to get near-bed orbital wave characteristics and sediment-transports from this data, research results, a discussion of the used methods and results, conclusions and an appendix.

3.1. Context

The Dutch coast is a sandy coast located in the North Sea region. The Netherlands is a country partly below Amsterdam Ordnance Datum (NAP), which needs to be protected from flooding by hard and soft coastal structures, such as dunes and dikes. Since 1990, the Dutch government favours soft coastal defence measures over hard structures. Therefore, sand nourishments are applied. The third coastal memorandum (3e Kustnota) describes how sand-nourishments are used to maintain a reference coastline (the 'Basiskustlijn') and the so-called coastal foundation.
In the 'Nota Ruimte' (VROM, 2004), the coastal foundation is defined as follows:

"The coastal foundation covers the entire sandy area, wet and dry, which as a whole is important as carrier of functions in the coastal area.
The coastal foundation is confined as follows:

- The seaward boundary consists of the continuous NAP -20m contour
- On the landward side, the coastal foundation comprises all dune areas and all the hard sea defences located on them. In the case of narrow dunes and dikes, the landward boundary coincides with the boundary of the flood defence, extended with the spatial reservation for 200 years of sea level rise and, where the dunes are wider than the flood defence, covers the entire dune area.

In the southwest and northeast, the coastal foundation is confined by the Belgian and German border of the Dutch continental shelf. The Wadden Sea and the Western Scheldt are not part of the coastal foundation.

The seaward boundary of the coastal foundation is the -20m NAP water depth contour. The 3rd Kustnota describes the current coastal defence policy and assumes that the sediment transport over this NAP -20 m contour is negligibly small (see also Mulder, 2000). Calculations on sediment demand within the Dutch coastal system and sea level rise led to the current policy in which annually approximately 12mln m^3 sand is nourished to maintain the coastal foundation and to maintain the coastline. Although the amount of sediment transport might be negligible, sediment transport does take place. A net sediment transport into the coastal foundation has effects on the sediment-balance of the coastal foundation.

In their literature review on the Dutch lower shoreface, Van der Werf et al. (2017) conclude that "The importance of offshore turbulence asymmetry streaming up- and downwelling on cross-shore sand transport has not yet been quantified. Furthermore, it is unclear how cross-shore tidal current components contribute to on- and offshore sand transport."

Rijkswaterstaat, the executive agency of the Dutch Ministry of Infrastructure and Water Management, started a research project called Coastal Genesis 2.0 to answer the following three research questions:

- How much sand will be needed in long term to ensure that our coastal foundation keeps pace with sea-level rises?
- Where and when will that sand be needed?
- And what is the best way to add this to the coast? (Min I&W, 2017)

The collected knowledge enables optimising the maintenance and management of the Dutch sandy coast. This will be implemented in a new sand nourishment policy in 2020 (Min I&W, 2017)

One of the modes of sediment transport is bed-load transport induced by orbital flow velocities and mean currents. The latter topic will be subject of research by others (Leummens, in prep.). The effects of orbital flow velocity on bed-load sediment transport in the nearshore are extendedly researched by amongst others Ruessink et al (2012) and Abreu et al (2010). When waves approach the shore, they become skewed. Skewed waves have a higher forward than backward velocity, generally resulting in a sediment transport that is shoreward directed. Chapter 5 will go into more detail on this subject. This thesis focusses on sediment-bed load transport on the lower shoreface, because the knowledge on morphological processes in this area is limited. Coastal Genesis 2.0 is one of the first research projects which gather flow velocity data in this area. The middle shoreface is "the zone between approx. the NAP -8 m and NAP -20 m depth contours with typical bed slopes between 1:200 and 1:1000, and where sand ridges may be present." (Van Rijn, 1998). In line with other papers, such as Browning, et al (2006), this area is called 'lower shoreface' in this thesis report.

In morphodynamic models such as Unibest and Delft-3D, the bed-load transport formulations by Van Rijn (2007) are often used to calculate the bed-load transport. These formulations use a parameterized intra-wave velocity signal that requires significant wave height, wave spectral peak period and water depth as input. Practical parameterizations are those from Isobe & Horikawa (1982) or Ruessink et al (2012).

This research compares measured orbital flow velocities on the lower shoreface with orbital flow velocities calculated with parameterizations, and how both measured velocities and calculated velocities with parameterizations affect the calculated bed-load sediment transports.

3.2. Research aim and research questions

The literature review by Van der Werf, et al. (2017) deduced two research problems concerning the sediment transport on the lower shoreface:

- There is a lack of knowledge on wave-induced current processes on the lower shoreface and their impact on sediment transport.
- There is a lack of knowledge on orbital wave motion on the lower shoreface and the ways to use the wave orbital motion as input in a quasi-steady bedload formula to calculate transport rates.

This research tries to contribute to the knowledge needed to solve the problem on the lack of knowledge on orbital wave-motion stated in the previous paragraph. In this study computed orbital flow velocities based on parameterizations by Isobe & Horikawa (1982) and Ruessink et al (2012) are compared with measurements. With the computed and measured velocities bed-load sediment transport rates are computed. The aim of this research is to find an answer to the following question:

What is the potential bed-load sediment transport on the Dutch lower shoreface, due to orbital wave motion?

The following sub-questions are used to find an answer to this question:

1. *What are the near-bed wave characteristics measured on different locations on the lower shoreface?*
    a. *Wave orbital velocity magnitude*
    b. *Wave orbital velocity skewness and asymmetry*

2. *How do measured orbital velocities, skewness and asymmetry on the lower shoreface compare to calculated orbital velocities by the parameterization proposed by Isobe & Horikawa (1982) and the parameterization by Ruessink et al (2012)?*

3. *What is the influence of water depth on bed-load sediment transport on the lower shoreface due to orbital wave motion?*

4. *What is the influence of grain size of sediment on sediment movement on the lower shoreface due to orbital wave motion?*

5. *What is the potential bed-load sediment transport on the Dutch lower shoreface due to orbital wave* motion?
    a. Using the flow velocities from the Isobe & Horikawa and Ruessink parameterizations;
    b. Using the measured flow velocities?

4. Theoretical Background

To answer the posed research questions, theoretical background is needed. To answer the first question about the near-bed orbital wave motion, the theoretical definitions on that subject are explained first. The theory behind the parameterizations, mentioned in the second sub-question and the theory behind calculating bed-load sediment transport, using the Van Rijn (2007) formulations are discussed as well. This theory is needed to calculate bed-load sediment transports.

4.1. Near-bed orbital wave characteristics

In deep water, waves generally have a sinusoidal shape. As waves propagate from deep water into shallower water, the shape of the wave orbital motion become increasingly non-linear. Initially, the waveform becomes asymmetric about the horizontal axis, with shorter, higher crests and longer, shallower troughs. This type of asymmetry is known as skewness. Closer to the shore in the shallower water of the surf zone, the asymmetry about the horizontal axis changes into asymmetry about the vertical axis as the waves increasingly pitch forward, with a steep front face and a gentle rear face. This type of non-linearity is referred to as asymmetry. Figure 1 illustrates these different wave shapes.

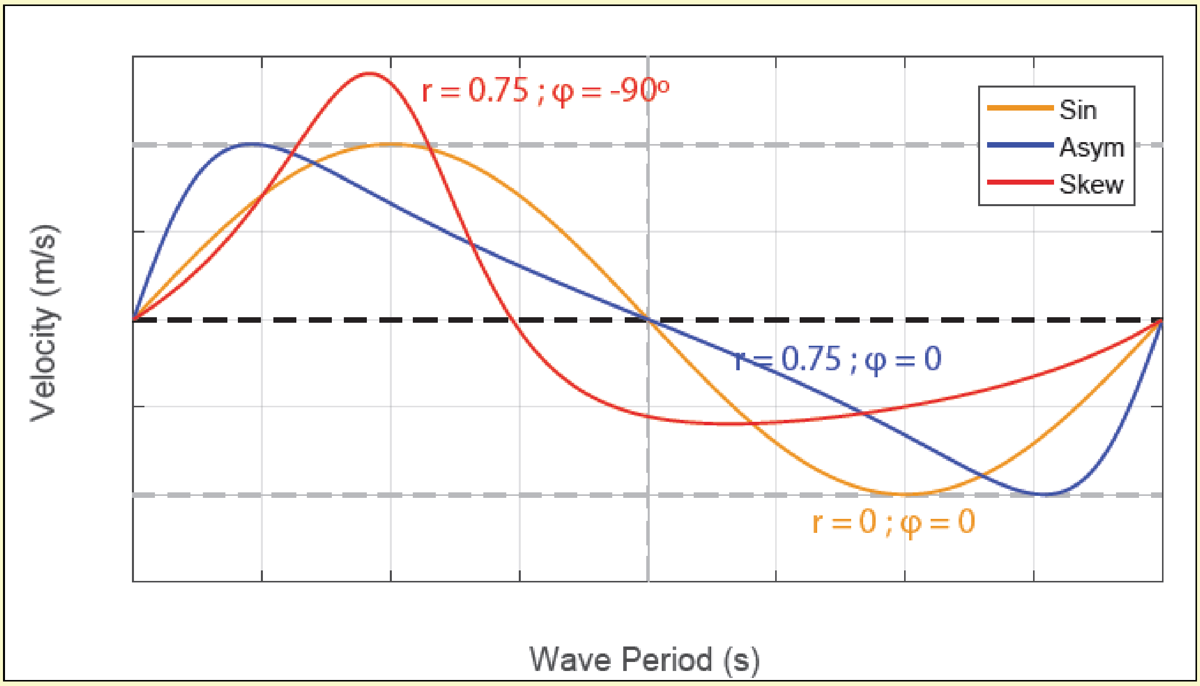

Figure 1 - Sinusoidal, asymmetric and skewed wave. Adapted from Albernaz et al. 2018

Different measures exist to evaluate if a wave is skewed and/or asymmetric. Figure 2 shows an example of the velocity and acceleration time series within one wave period (Malarkey and Davies, 2012) This wave is skewed, as its maximum forward velocity U_{max} is higher than its maximum backward velocity U_{min}. The wave is also asymmetric, as its maximum forward acceleration a_{max} is higher than its maximum backward velocity a_{max}. at t=0, the velocity time series cross the u=0 line positively, this is called the zero-upcrossing. At $t_{0,}$ the line is crossed again at the zero-down crossing.

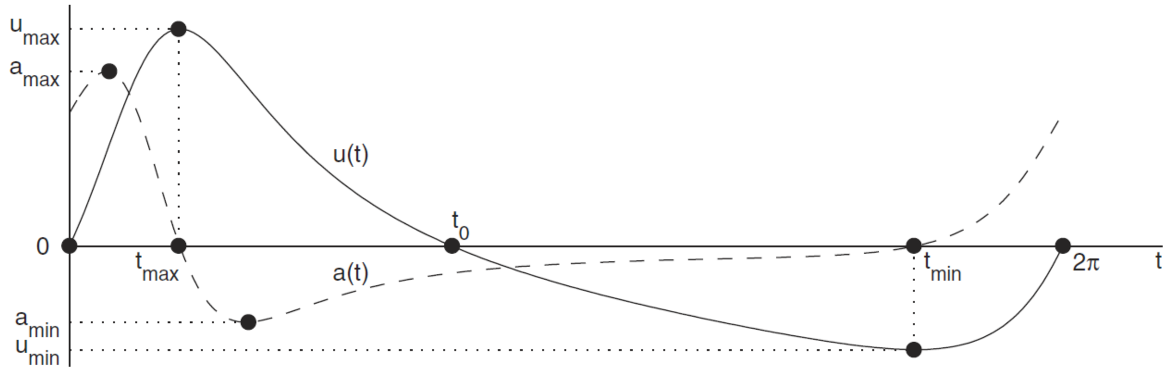

Figure 2 - Definition sketch of the non-dimensional free-stream velocity u and acceleration a time series beneath asymmetric skewed waves (Malarkey and Davies, 2012)

Skewness and asymmetry can be quantified in different ways. Abreu et al (2010) use the indicators R and β:

$R_u = \frac{u_{max}}{u_{max} - U_{min}}$ (Skewness) (1)

$\beta = \frac{a_{max}}{a_{max} - a_{min}}$ (Asymmetry) (2)

In which u_{max} and u_{min} are the maximum and minimum forward orbital velocities, and a_{max} and a_{min} the maximum and minimum orbital accelerations (See Figure 2).
A completely non-skewed symmetric wave yields R=0,5 and β=0,5.
The abbreviations u_{max}, u_{min}, a_{max} and a_{min} are often used in literature about orbital wave motion. In this research, u_{for}, u_{back}, a_{for}, a_{back}, with the same definitions are used, to highlight that maximum positive velocity is reached while waves move forward.
Ruessink et al (2012) use the following slightly different method for determining the skewness and asymmetry in velocity time series:

$S_u = \frac{\mathrm{mean}(u_w^3(t))}{\sigma_{u_w}^3}$ (Skewness) (3)

$A_u = \frac{\mathrm{mean}((\mathbb{H}(U_w(t)))^3)}{\sigma_{u_w}^3}$ (Asymmetry) (4)

In which $\mathbb{H}(U_w(t))$ is the Hilbert transform of $U_w(t)$. U_w is the wave velocity and $U_w(t)$ is the wave velocity as function of time. σ_{uw} is the standard deviation of $u_w(t)$. Using the β-parameter, a positive asymmetry describes a forward leaning wave, using the A_u-parameter, a negative asymmetry describes a forward leaning wave (Ruessink et al, 2012).

According to Abreu (2011) "[…] It is noted that the final purpose of the previous definitions [of skewness and asymmetry measures] is the same. All of them intend to
characterize nonlinear wave properties through the identification of the velocity and acceleration skewnesses, which are recognized to be inextricably linked to the movement of sediments.". The R_u and β parameters are easier to calculate for standard velocity profiles for regular waves, while the S_u and A_u parameters give a more complete view on asymmetry and skewness for irregular waves, because it uses an entire velocity profile and not only the maxima and minima in the wave shape.

4.2. Parameterizations by Isobe & Horikawa and Ruessink

Different calculations and deterministic models exist for calculating the intra-wave velocity profile. In deep water, linear wave theory, in which the velocity profile is considered sinusoidal is widely used. However, when waves are entering the near-shore, this sinusoidal representation does not cover the wave skewness and asymmetry. Advanced deterministic wave models, using Boussinesq or Reynolds-Averaged Navier-Stokes equations provide accurate descriptions of near-shore wave orbital motion, but are computationally demanding. Therefore, parameterizations are used in numerical modelling.

Isobe & Horikawa (1982) and Ruessink et al. (2012) propose parameterizations to describe wave orbital motion, including skewness and asymmetry. These parameterizations take significant wave height, wave (peak) period and water depth as input. The significant wave height is the mean height of the highest 33% of the waves in a chosen period (Van Rijn, 2013). The wave spectrum peak period is the period in which the wave energy spectrum has the highest energy. The parameterizations compute the forward and backward horizontal flow velocities.

The mathematical representation of the Isobe&Horikawa-parameterization (further in this report sometimes abbreviated as IH-parameterization) and Ruessink parameterizations are presented in appendix A. A conceptual representation of the calculation steps involved in both parameterizations is shown below.

Isobe & Horikawa

Both parameterizations determine the amplitude of velocity $\hat{U}_w$ according to linear wave theory first (Figure 3):

$$\hat{U}_w = \frac{\pi H_s}{T_p \sinh(kh)} \quad (5)$$

In which:

H_s = significant wave height in m

T_p = peak wave period in s

h = water depth in m

k = wavenumber in m^{-1}

The wavenumber could be found by solving the dispersion relation in linear wave theory:

$$\left(\frac{2\pi}{T}\right)^2 = gk\tanh(kh) \quad (6)$$

In which

T	wave period (s)
g	gravitational acceleration (m/s^2)
k	wave number (rad/m) (=spatial wave frequency)
h	water depth (m)

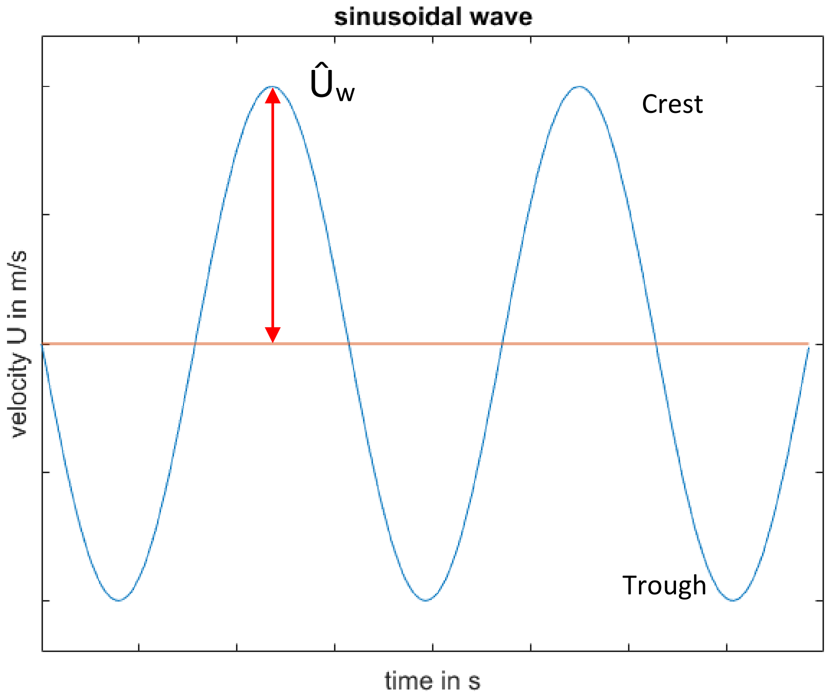

Figure 3 - Orbital wave amplitude of velocity in linear wave theory

With this value, the Isobe & Horikawa parameterization uses correction parameters to find the skewed forward and backward maximum velocity and crest and trough wave phases. In this research, the Van Rijn (2007) application of the Isobe & Horikawa parametrization is used in which the wave shape is constructed using two sinusoidal half waves, based on the found (skewed) crest- and trough velocity amplitudes (Figure 4). See Appendix A for further details.

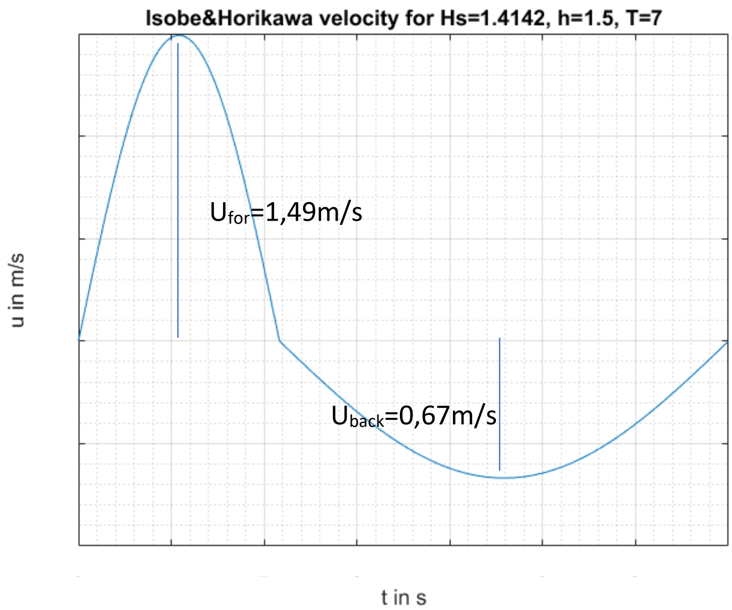

Figure 4 - Isobe & Horikawa waveshape with discontinuity

Ruessink

Abreu et al (2010) presented another parameterization with the same input values, but other parameters, based on waveform and phase of rotation (r and φ). In this way a continuous parameterization was obtained, which includes both velocity skewness and asymmetry:

$$U_t = \hat{U}_w\sqrt{1-r^2}\,\frac{\sin(\omega t)+\frac{r}{t-\sqrt{1-r^2}}\sin\varphi}{1-r\cos(\omega t+\varphi)} \qquad (7)$$

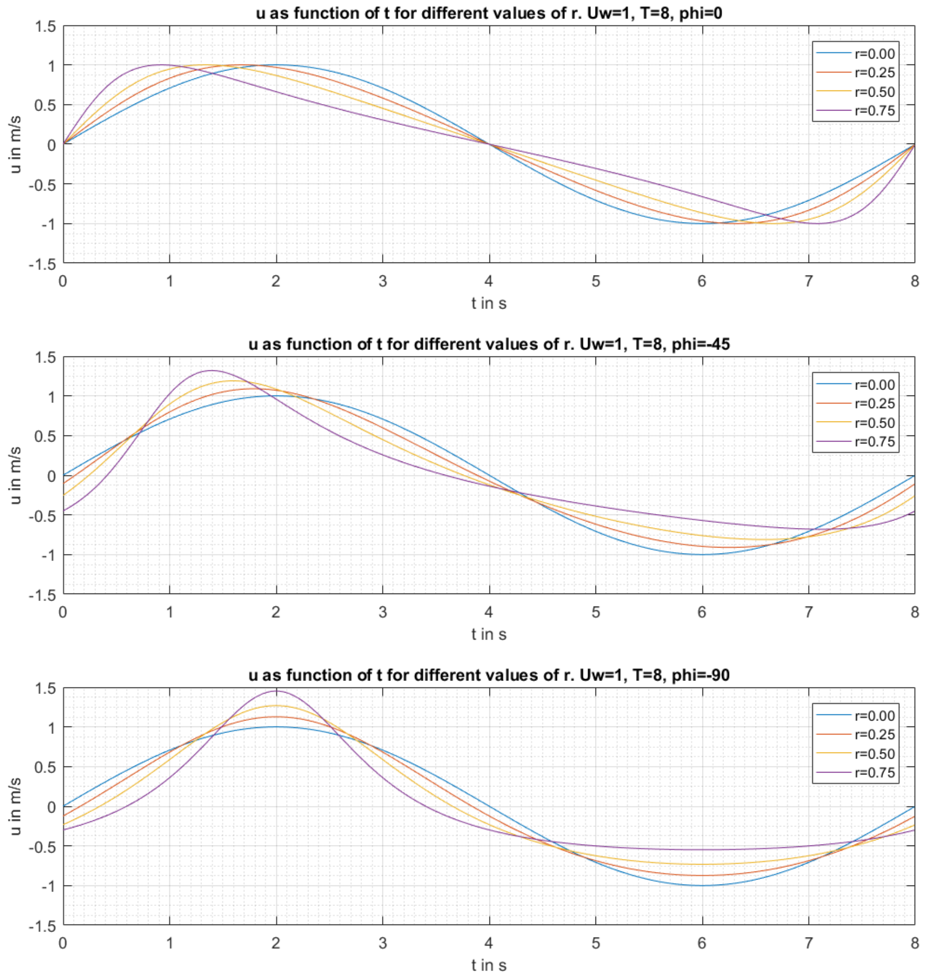

Figure 5 - using different r & phi parameters in the Abreu parameterization

Varying the r and φ parameters leads to different waveshapes, as shown in figure 5. A waveshape with r=0 and φ=0° is sinusoidal. Asymmetric velocity signals are obtained for φ=0 and φ=-45° with r=0.25, 0.50 and 0.75, where a higher r results in a higher asymmetry. Saw-tooth wave with high asymmetry result from φ=0° and r=0.75. Skewed velocity signals are obtained for φ =-90° with r=0.25,0.50 and 0.75. A higher r-value results in a higher forward peak velocity.

Determining the parameters r and φ presented in the Abreu parameterization from skewness and asymmetry indicators is rather cumbersome according to Malarkey & Davies (2012), as it requires quartic equations to be solved. Ruessink et al. (2012) found a better way to fit the parameters for the proposed parameterization, using the Ursell Number:

$$UR = \frac{3\,H_s\,k}{8(kh)^3} \qquad (8)$$

In which H_s is the significant wave height (m), k the wave number (rad/m) and h the water depth (m). Ruessink et al. (2012) proves empirically that there is a relation between the Ursell Number and skewness S_u and Asymmetry A_u (Figure 6). Malarkey and Davies (2012) give the relation between φ and A_u and S_u and r and A_u and S_u. With this information, r and φ could be linked directly with the Ursell number.

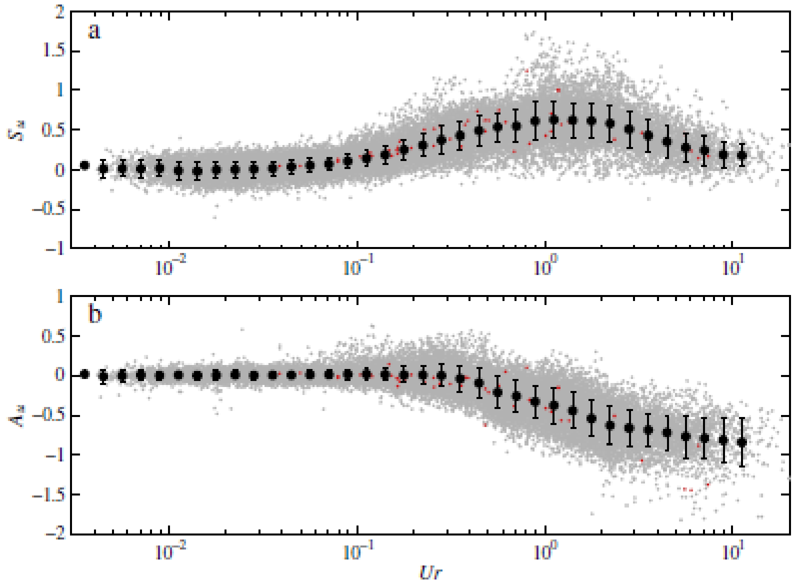

Figure 6 - Near-bed velocity skewness Su and (b) asymmetry Au as a function of the Ursell number Ur. (Ruessink et al. 2012)

The equations for the Ruessink parameterization are presented in Appendix A.
Ruessink et al. (2012) applied this parameterization to near-shore conditions and shows good agreement with observations. It is yet unclear if it is applicable in lower shoreface circumstances.

The difference between the two parametrizations can easily be seen for a relatively small water depth of 1.5 m (figure 7). At this water depth, the Ruessink parameterization yields a larger orbital velocity amplitude than the Isobe-Horikawa parameterization. The Isobe&Horikawa parameterization shows a more skewed wave than the one by Ruessink et al (2012), which is in line with the findings of Ruessink et al. (2012). As the Van Rijn (2007) application of the Isobe&Horikawa parameterization uses two half sinusoidal waves, it shows no asymmetry, as its forward and backward accelerations are the same. Abreu et al. (2010) argues that the parameterization results in flow accelerations which are discontinuous and therefore not appropriate to use directly in models. This is also clear from the lower plot in figure 7.

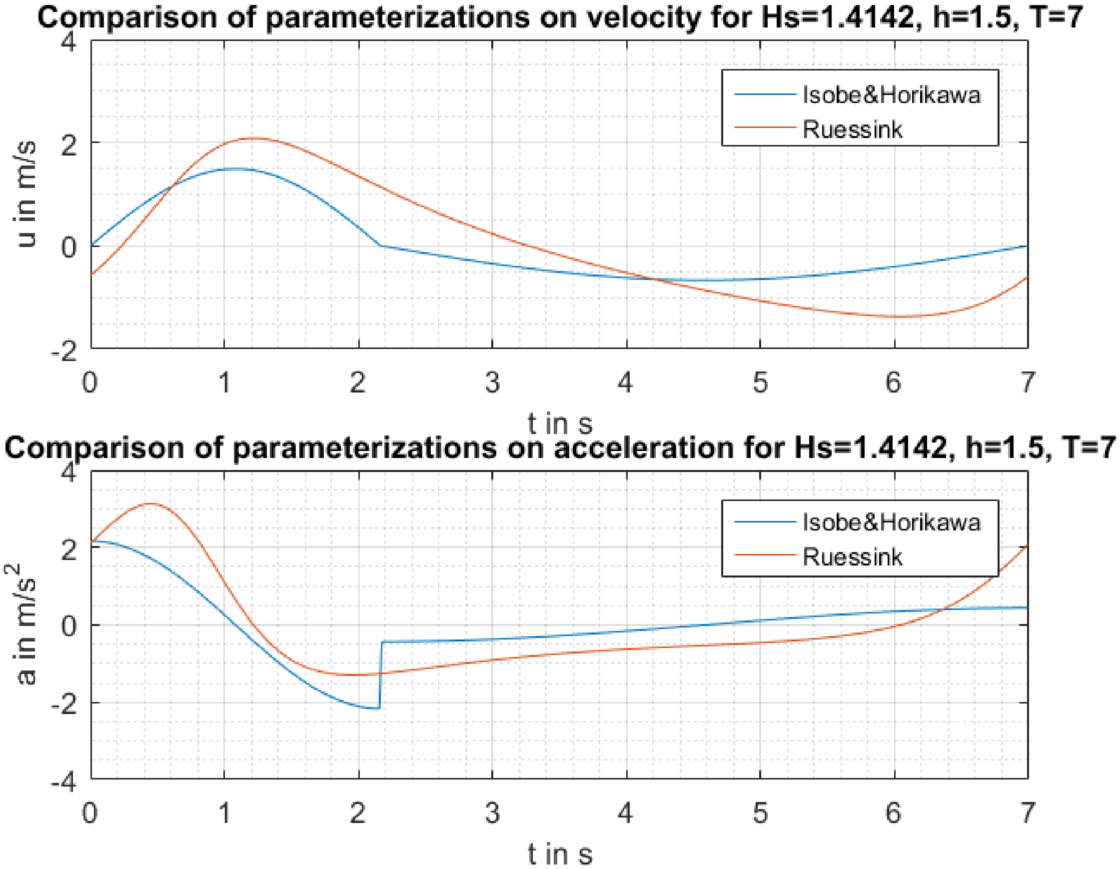

Figure 7 - Comparison of parameterizations on velocity and accelerations for low water depth

4.3. Bed-load transport

Bed-load sediment transport on the lower shoreface depends on wave height and direction, water depth, current magnitude and direction, sediment size etc. Van Rijn (2007) proposes an engineering method to compute the bed-load transport rates. The method is "fully predictive in the sense that only the basic hydrodynamic parameters depth, current velocity, wave height, wave period, etc. and the basic sediment characteristics d10, d50, d90, water temperature, and salinity need to be known. The prediction of the effective bed roughness is an integral part of the model." (Van Rijn, 2007).

The fully predictive calculation takes surface wave characteristics peak wave period and significant wave height as input and calculates the forward and backward orbital velocities using the Isobe & Horikawa parameterizations. For this research, the Isobe&Horikawa parameterization was removed, so that the direct input for the bed-load sediment transport formulations are the forward and backward orbital velocities instead of significant wave height. In this way, the impact of using the Isobe&Horikawa parameterization, Ruessink-parameterization and measured orbital velocities on bed-load transport could be compared.
Figure 8 schematically shows the dependencies in the Van Rijn (2007) formulations.

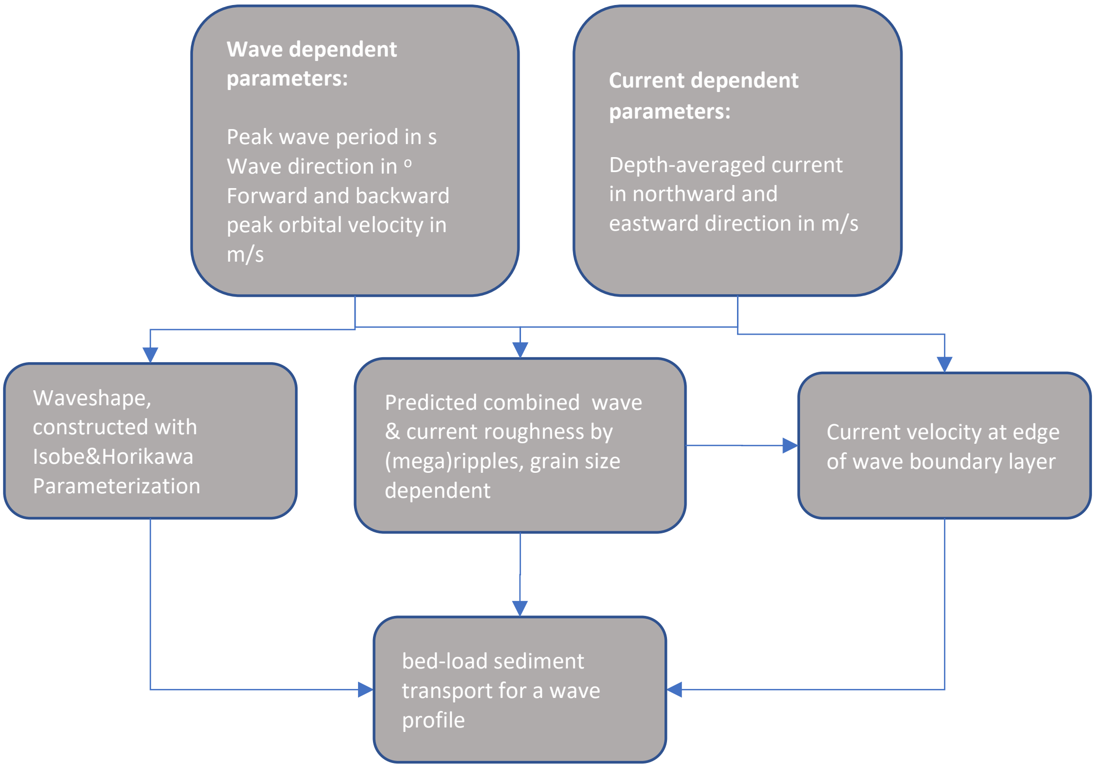

Figure 8 - Simple conceptual model for Van Rijn (2007) bed-load transport calculation

Constants, which are not included in this brief conceptual model, ae water and sediment densities, the Von Kármán constant, salinity and gravitational acceleration. Those parameters, the way they affect the calculation of bed-load transport and the calculation itself are precisely described by Van Rijn & Walstra (2004).

Within the Van Rijn (2007) bed-load calculation, the peak wave orbital velocity $\hat{U}_w$ in m/sand peak wave orbital excursion a_b in m are determined as follows:

$$\hat{U}_w = \frac{\pi H_s}{T_p \sinh(kh)} \tag{9}$$

$$a_b = \frac{H_s}{2 * \sinh(kh)} \tag{10}$$

From these formulas it follows that:

$$a_b = \frac{\hat{U}_w T_p}{2\pi} \tag{11}$$

The wave orbital velocity can be directly determined from a velocity signal. Equation 11 can be used to find a_b, without knowing H_s.

Mean currents and orbital wave velocities may have different directions. Figure 9 shows how the sediment bed-load transport vector is built up. For a time-dependent wave velocity within one wave period, the flow velocity of the wave and the current are combined into a vector in which direction the sediment is transported. Note that the wave direction H_{dir} is opposite to the direction of the wave-component of the bed-load H_{dirto}.
The north and east components of the vector of the bed-load are integrated over time for one wave period.

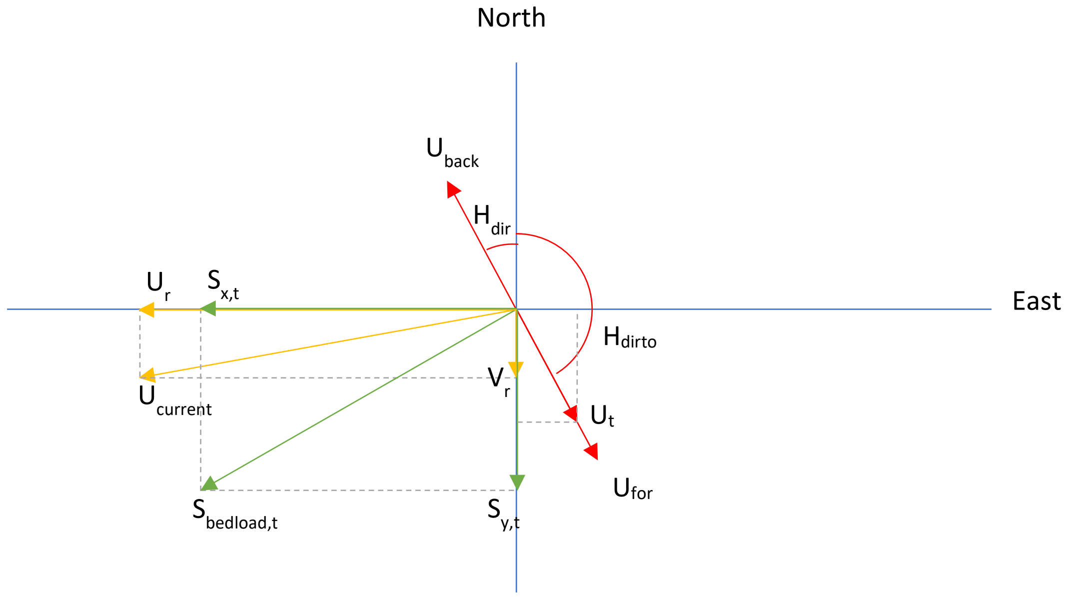

Figure 9 - Directions in Van Rijn (2007) bed-load calculations

5. Data availability - Flow, waves and sediment data

In this chapter, the available data used to answer the research questions posed in the previous chapter and the extent to which it could be used is discussed. To find answers on the research questions, data is used from different data sources. This chapter described the used data on near-bed orbital flow velocities, surface wave characteristics and sediment grain sizes.

5.1. Near-bed flow velocities

Instrumented measurement frames were installed at the lower shoreface offshore of the Ameland tidal inlet in the autumn of 2017 (See Figure 10 and Table 1) as part of the Coastal Genesis 2.0 research programme. The measurement frames carry different sensors to measure flow velocities, currents, suspended sediment concentrations and bed morphology. Data from the many and diverse measurements should ensure validation of morphodynamical models used by Rijkswaterstaat, and further calibration and optimisation of the data can enable more accurate ‘prediction’ of effects of changing weather influences (Min I&W, 2017). In this study, data is used from the acoustic doppler velocimeters (ADV’s) mounted on two of these frames and deployed at NAP-16 m and NAP-10 m (See Figures 12 and 13 for the arrangement of the ADV’s on a measurement frame).

Figure 10 - Locations of measurement frames from Coastal Genesis 2.0

Frame	Depth (-m NAP)	Sensors	Measurement volume height (m above bed)	RD-coordinates	degrees, minutes, seconds	Start timeseries	End time series
1	20	ADV01	0.488	168339, 615736	N 53 31 39.2, E 5 35 18.1	08-11-2017 14:00	28-11-2017 04:30
		ADV02	0.189			08-11-2017 14:00	28-11-2017 07:30
3	16	ADV05	0.494	168449, 613779	N 53 30 35.9, E 5 35 23.7	08-11-2017 12:00	11-12-2017 14:30
		ADV06	0.194			08-11-2017 12:00	16-11-2017 13:30

Table 1 - Measurement frame information

The sensors are attached on different heights on the frames (Table 1), Every half hour, the sensors measure a so-called ‘burst’ with velocity measurements. Each burst contains 28640 measurements, with a frequency of 16 Hz. The ADV’s measure velocities 15,7cm below the ADV sensor the flow velocity in x, y and z-direction (Figure 11).

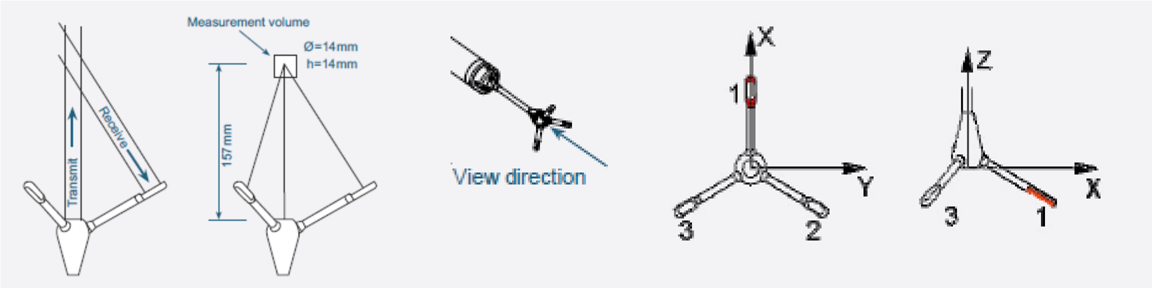

Figure 11 - Measurement volume and x,y,z-coördinates *(Nortek AS, 2005)*


Figure 12 - Measurement frame (Mol, 2017)


Figure 13 - Arrangement of ADV's (Mol, 2017)

5.2. Surface wave characteristics

Besides velocity data also wave information is required as input to compute sediment transport rates. Wave information is herein obtained from a so-called wave transformation matrix.
The Deltares wave transformation Matrix transforms amongst others the measured wave period, significant wave height and wave direction measured on offshore measurement stations to arbitrarily chosen coordinates somewhere in the Dutch coastal area (Fockert & Luijendijk, 2011). In the case of the Amelander Zeegat, the measurement stations at the Eierlandse Gat and Schiermonnikoog are used.

In this research, the coordinates of the measurement frames, listed in Table 1 are chosen as output locations for the transformation matrix. Near the measurement frames, different Rijkswaterstaat wave buoys measure the peak wave period, wave direction and significant wave height as well. To validate the transformation matrix, the coordinates of one of these wave buoys (Amelander Zeegat boei 1-1) are chosen as output locations for the transformation matrix (See Figure 14 for map) and compared with the output of the buoy in the period between 1 November and 15 December 2017 (see figure 15).

Figure 14 - Location wave buoy for validating transformation matrix

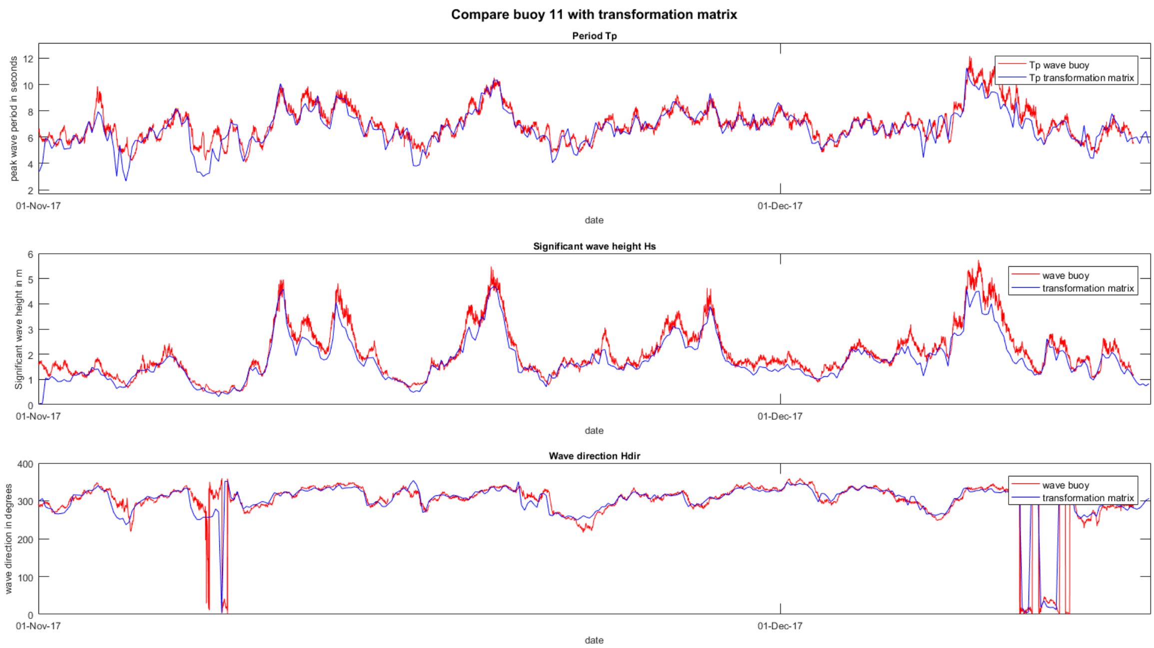

Figure 15 - Validation transformation matrix with measurement buoy

In the upper plot in Figure 15 the peak wave period is shown for both the wave buoy and the transformation matrix. The transformation matrix shows low period outliers compared to the wave buoy, but the peak wave periods are well comparable.
The significant wave height from the transformation matrix shows the same low outliers. Because these outliers don't occur on high-energy events, their impact is assumed to be small. The wave direction does resemble very well. At first sight, some dips could be seen in the lowest plot, but keeping in mind that 361° is equal to 1°, this is acceptable.

In the Figure below, the peak wave period, significant wave height and wave direction data from the transformation matrix between 1 November and 15 December 2017 on both measurement frame locations are shown.

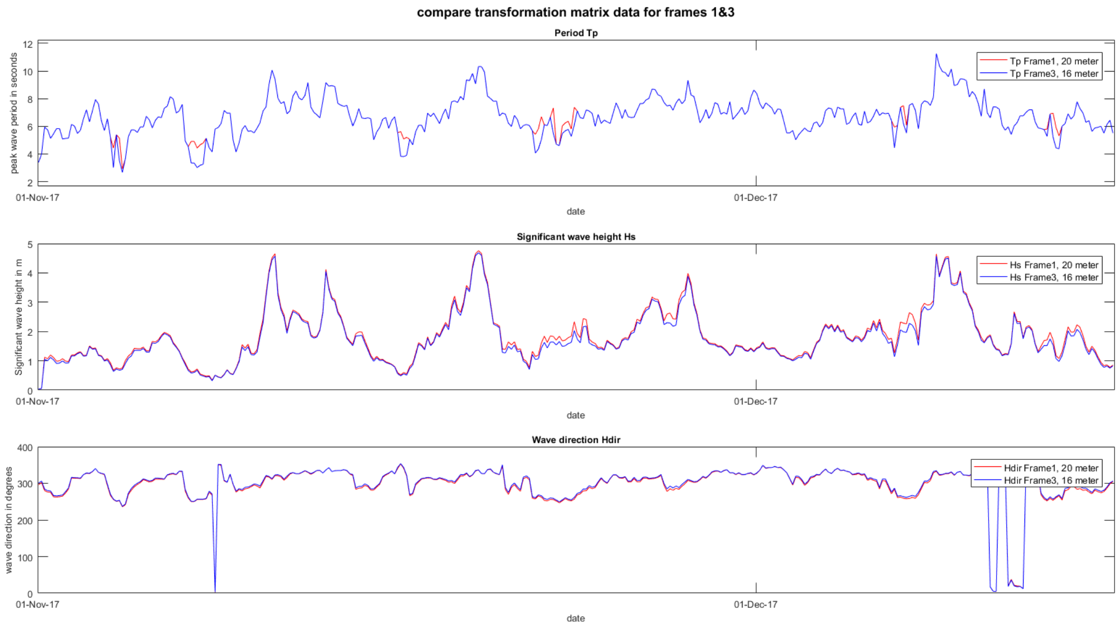

Figure 16 - Comparison transformation matrix data for frames 1&3

	Frame 1 (20m)	Frame 3 (16m)
Min Hs (m)	0,04	0,04
Max Hs (m)	4,8	4,7
Mean Hs (m)	1,9	1,8
Min Tp (s)	2,9	2,7
Max Tp (s)	11,3	11,3
Mean Tp (s)	6,8	6,7

Table 2 - Hs and Tp values from transformation matrix between 01-09-17 and 15-12-17

Figure 16 clearly shows a few energetic events in the wave data. Four events have higher significant wave height than 4m, on 10 November, 4,65m was observed, 4,12 meters was observed on 13 November, 4,8m was observed on 19 November and 4,56m was observed on 9 December.

The wave direction is usually NNW, which is almost perpendicular to the coastline. The mean significant wave height at frame 1 is with 1,85 m only 0,08 m higher than the mean significant wave height of 1.50 m at frame 3. The decrease in significant wave height between the two measurement frames is expected to be caused by breaking of waves. The wave direction on both locations is almost the same. The mean peak wave period at frame 1 is also slightly higher than the peak wave period at frame 3 (Table 2).

5.3. Sediment grain size

On different locations near the measurement frames, sediment samples were taken on the fourth of July in 2017, see Figure 17. Samples BC-28-AA and BC-30-A are the nearest samples to measurement frames one and three respectively.

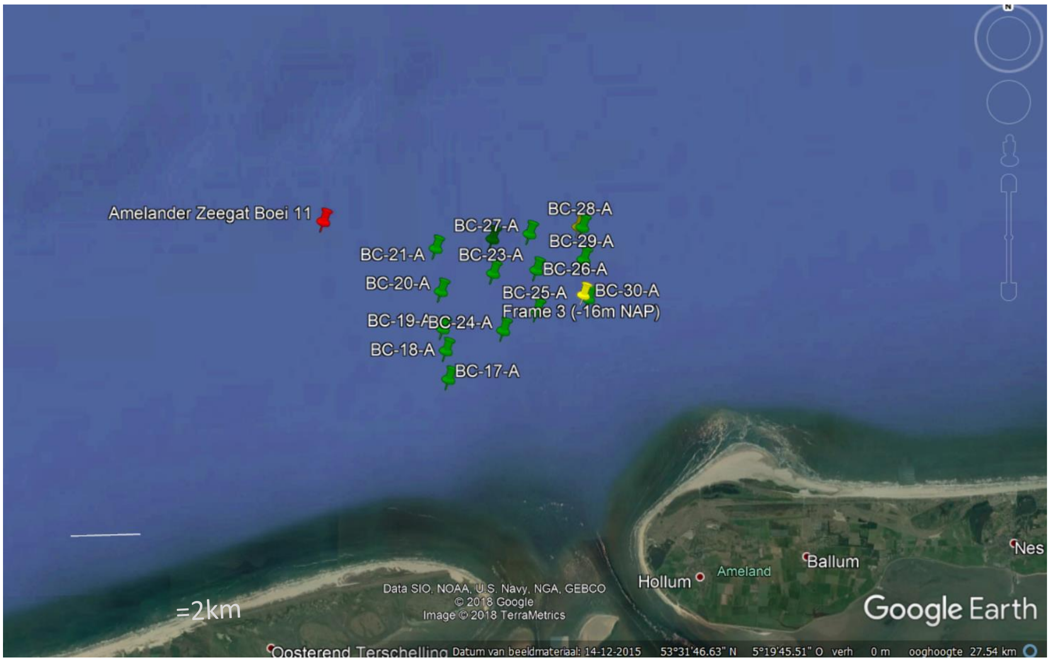

Figure 17 - locations of sediment samples

The values of the two samples near the measurement frames and the maximum and minimum values of all sediment data are listed in Table 3 and plotted in Figure 18.

	D10 in µm	D50 in µm	D90 in µm
BC-28-A	155	216	298
BC-30-A	128	207	332
Min for all samples	105	186	289
Max for all samples	165	233	337
Mean for all samples	146	216	317

Table 3 - sediment grain size data

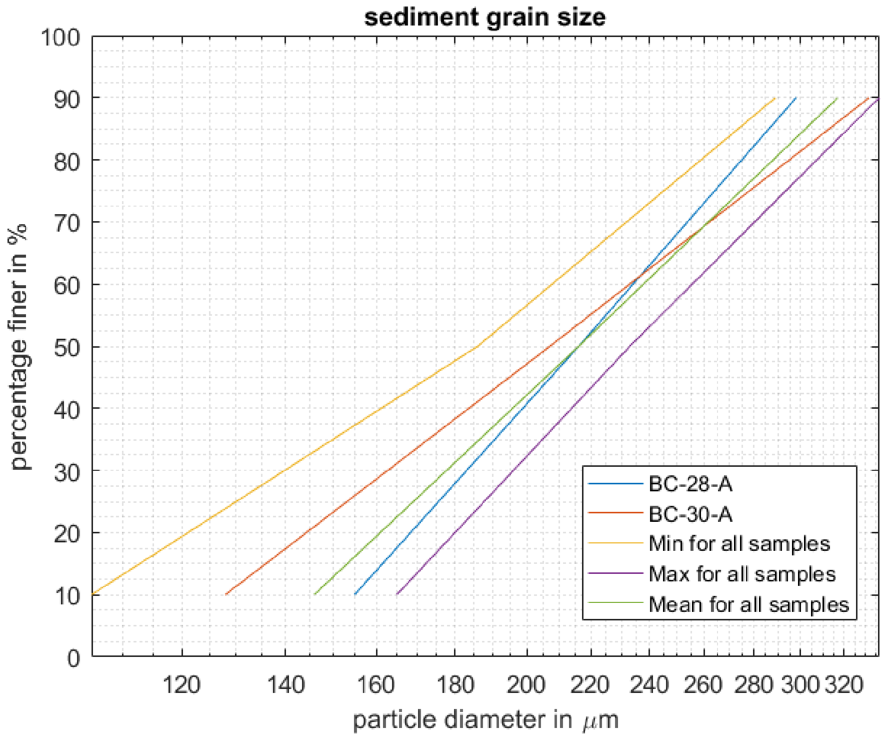

Figure 18 – sediment grain sizes in the area near the measurement frames

According to the Dutch soil classification system, the fraction between 105µm 210µm is called fine sand and the fraction between 210µm and 300µm is called moderately coarse sand. In calculating bed-load sediment transport, the sediment samples near the measurement frames will be used.

6. Methodology

The methods used to investigate the research questions stated are described in this chapter. Figure 19 illustrates the research process.

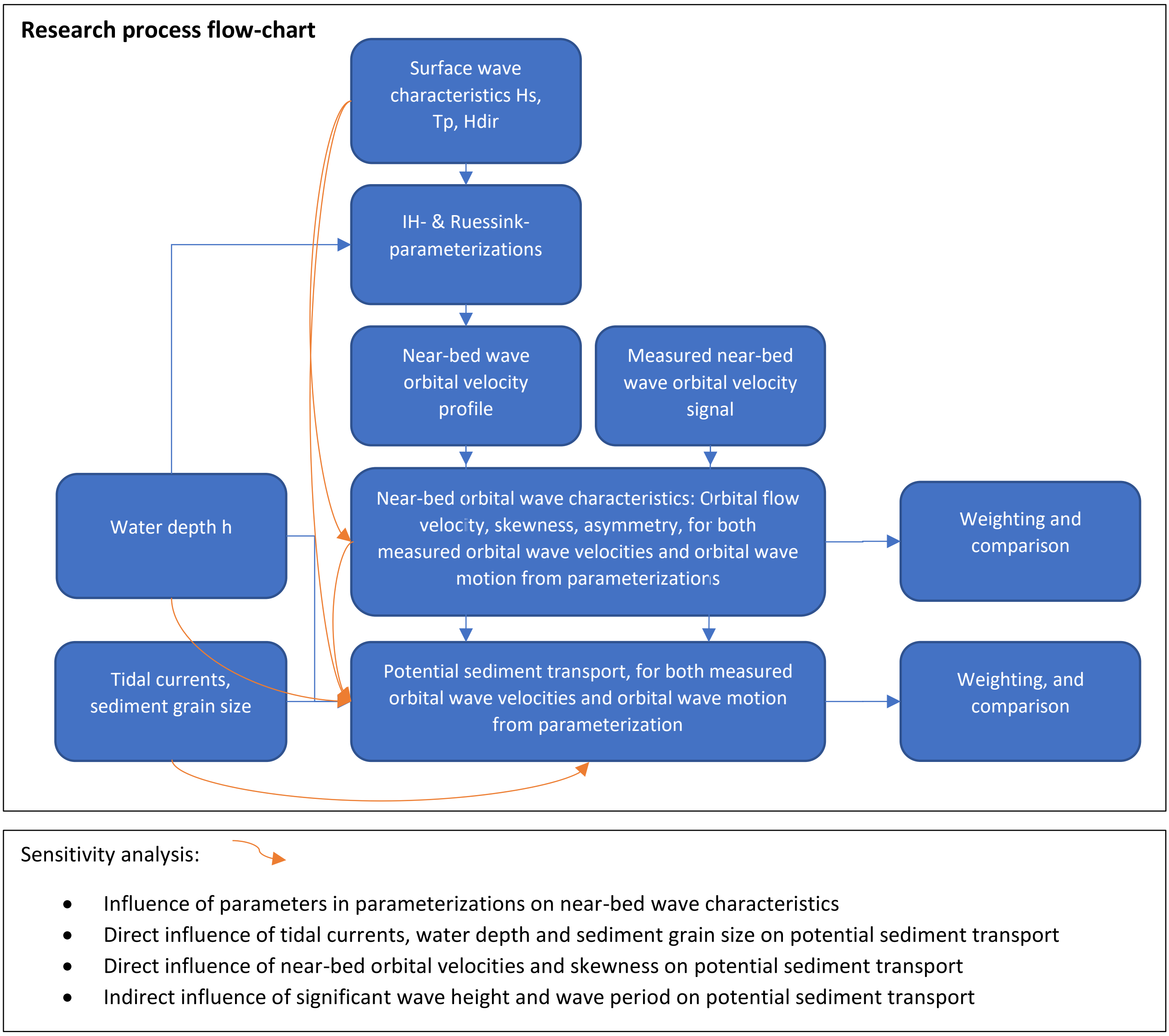

Figure 19 – Research process flow chart

First, the ADV-data is processed. Then, near-bed wave orbital characteristics from the measured velocity signal and parameterizations are calculated and compared to answer research questions 1 and 2. A sensitivity analysis is provided to estimate the influence of different parameters on the near-bed orbital wave characteristics, calculated with parameterizations. Afterwards, the calculation of bed-load sediment transport rates is presented. Sensitivity analysis determines the influence of both direct and indirect (via parameterizations) parameters on bed-load sediment transport (See Figure 19). The influence of direct parameters grain size and water depth is used to answer research questions 3 and 4. The last research question could be answered with the results of the comparison between sediment transport rates, calculated with parameterizations and with measured orbital velocities, the last process in this methodology.

6.1. Processing ADV-data to get an orbital wave velocity signal and tidal currents

Figure 20 shows the method used to process the ADV-data. The ADV-sensors supply a raw signal in x,y,z-direction. The axial system of these directions depends on how the ADV-sensors are arranged. Using the spatial arrangement of the ADV-sensors, the x,y,z-directions were translated to East, North, Up (ENU)-directions. Spikes and noise were removed from the raw ADV signals using the method by Goring and Nikora (2002).

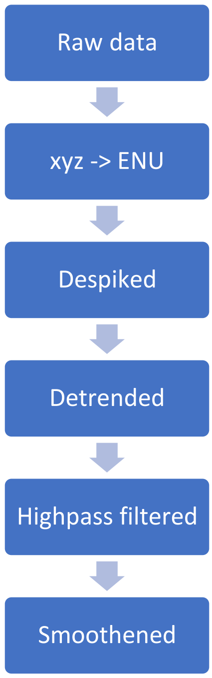

Figure 20 - Processing ADV-data flow chart

In analysing orbital wave characteristics, it is important that the tidal trends are removed from the data, such that the mean velocity is zero. This was done by subtracting the mean tidal current velocity from the signal per burst:

$$V_{detrend} = V_{signal} - V_{trend} \qquad (12)$$

A high pass filter was applied to filter out waves with a frequency higher than 0,05Hz (period of 20 seconds) from the data in the same way Ruessink et al. (2012) does to restrict the research to sea-swell waves, without infragravity waves.

The filtered data was smoothened using a moving average window of 25 sample values (about 1.6 seconds) to facilitate extracting wave peaks and troughs without turbulence peaks.

Waves and currents may have different directions. The ADV-data is described with an East- and North-component. Ruessink et al. 2012 uses Principle Component Analysis to find the principle wave direction and the component of the wave orbital velocity in the principle wave direction. In this research, the same principle for the high pass filtered signals is used, resulting in the principle wave direction and the orbital wave velocity in that direction per burst. The current direction is found by using Pythagoras for the mean trended signal during a burst in north and east direction.

Figure 21 shows an example of the detrended velocity signal for a 30-minute burst, with the northward velocity on the y-axis and the eastward velocity on the x-axis. The mean velocity in both directions is zero, because the trend was subtracted from the signal. In a principle component analysis, the two perpendicular eigenvectors of the complete matrix of signals are determined. The vector in which the signals have the smallest mean variance is the eigenvector in the principle direction. The angle of the principle eigenvector with the y-axis is the wave direction, in the case of Figure 21 this is 298°.

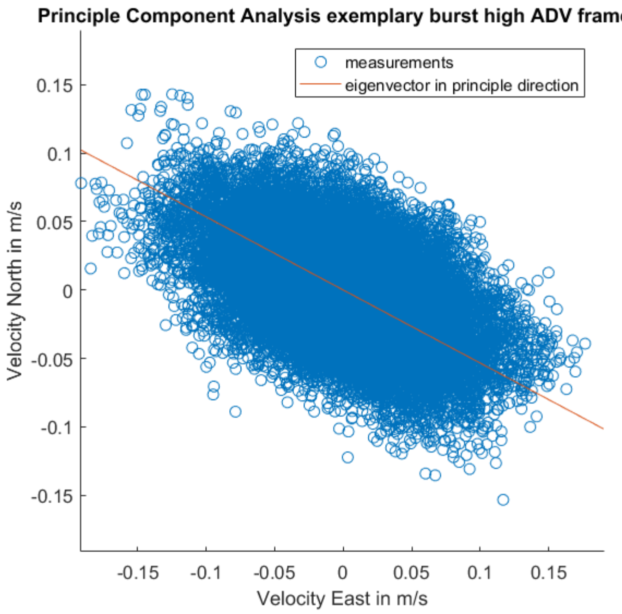

Figure 21 – Principle Component Analysis for an exemplary burst

6.2. Calculating near-bed orbital wave characteristics

The following near-be orbital wave characteristics are compared in this research:

- Significant for- and backward velocities. These follow directly from the processed ADV-data and Parameterizations
- Asymmetry and Skewness, calculated with equations 1,2,3 and 4.

6.2.1. Sensitivity analysis: Influence of parameters in parameterizations on near-bed wave characteristics

The influence of the significant wave height, peak wave period and water depth on significant forward orbital velocity, skewness and asymmetry is determined by a sensitivity analysis. This is done by keeping one parameter constant, while varying the others.

6.2.2. Near-bed wave orbital velocity signal from measurements

In this research default Matlab routines to assess the skewness Ru and asymmetry β from the velocity signals. In addition, dat2steep.m and dat2tc functions from the WAFO-toolbox of Lund University (the WAFO group, 2017) are used to find the zero-crossings and the peaks between these zero-crossings. Positive peaks are forward orbital velocity peaks U_{for} values and negative peaks are backward orbital velocity peaks U_{back}. The smoothened signal is used to reduce the zero-crossings due to turbulence. To show the effect of different smoothing windows, Figure 22 shows the peaks and troughs for one example burst and different smoothing windows. A time window of 25 timesteps leads to 57 found crests & troughs. A time window of 5 timesteps leads to 142 found peaks & troughs. This affects the resulting wave period (4.3 sec vs 10.6 sec) and mean U_{for} and U_{back} per burst. A smoothing window of 25 samples is pragmatically chosen, which comes down to about 1.6 s. Using this time-window, the surface wave characteristic Peak wave period is almost the same as the averaged measured wave period per 30 minutes.

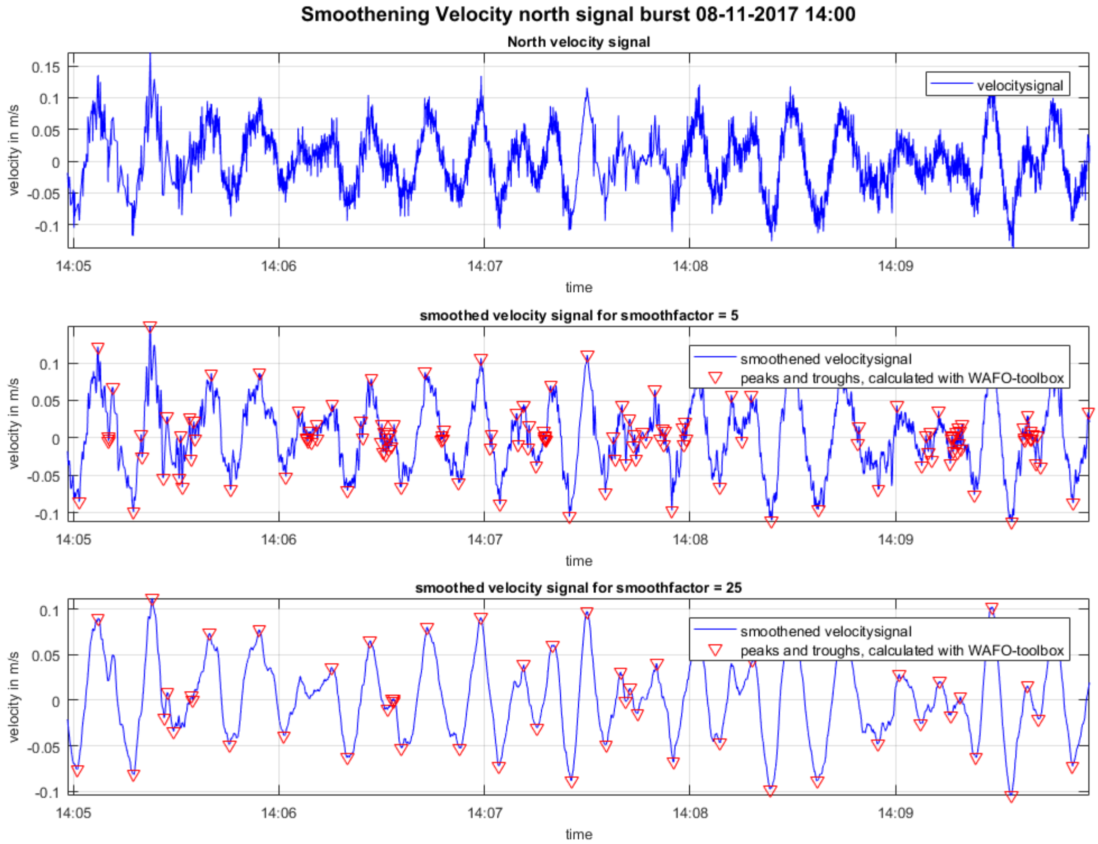

Figure 22 - Smoothening velocity signal (example)

The formulations proposed by Van Rijn (2007) use significant wave height as input. The significant wave height is defined as the mean wave height of the highest one third of all waves measured in a certain time series. Similarly, the significant orbital peak velocity was used to compute the bed-load transports. The significant orbital peak velocities per burst (30min time series) were determined as follows:

1. Find the 1/3 of the waves with the highest orbital diameter (U_{for} + U_{back} in m/s)
2. Determine the mean U_{for} and U_{back} of these waves
3. $\hat{U}_w$ is max ($U_{for,significant}$,$U_{back,significant}$)

The dat2steep.m routine was used to find the wave period per wave, the crest front speed and crest back speed (Figure 23), which is equal to the crest front acceleration and crest back acceleration for a velocity signal. These values were used to find the wave asymmetry β. Another way of determining the wave asymmetry, is with the Au-indicator, using the Hilbert-transform method in Equation 4.

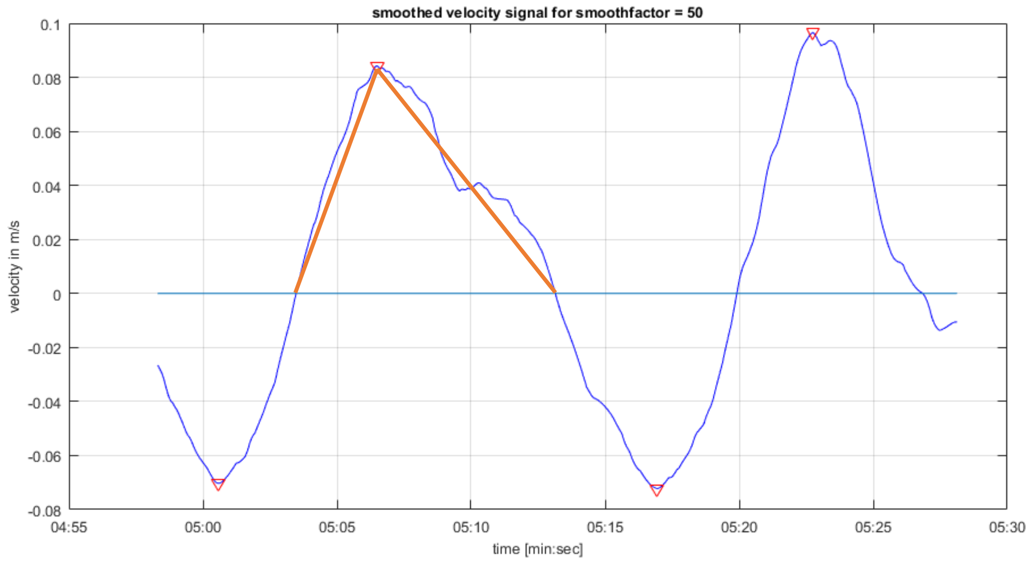

Figure 23 - Determining skewness & Asymmetry with peaks, troughs, zero-up crossings for a single wave (example)

6.2.3. Near-bed wave orbital velocity profile from parameterizations

It is easier to calculate the wave orbital velocity characteristics of the parameterizations. The parameterizations produce only 'standard' wave, instead of a velocity time series. The WAFO-tools used to find peaks and troughs are not needed. The forward and backward orbital velocities are extracted with standard Matlab tools, and the forward and backward accelerations are found by getting the maximum and minimum values in the derivative in the velocity profile, for example shown in Figure 7.

6.3. Calculation of potential bed-load sediment transport

The bed-load transport formula of Van Rijn (2007), described in paragraph 4.3 is used to calculate potential sediment transport for the ADV-data and the Isobe&Horikawa and Ruessink parameterizations using waves from the transformation matrix. The bed-load transport formula uses the depth-averaged current velocities U_r and V_r as input. The ADV-data is available for elevations of 0.2 m and 0.5 m above the bed. Theoretically, with current velocities at two different heights, an entire flow profile could be made using a simple logarithmic function. However, in practice a sample of only two heights is not large enough to construct a velocity profile with usable averaged current velocities. Data from another sensor, the ADCP could provide an entire flow profile, and is recommended to use in this case, but due to time limits in this research, the pragmatic approach of using the current signal of the upper ADV is chosen. This will most likely result in lower current velocities than the depth-averaged current velocities.

It is interesting to look at the potential sediment transport without currents first, to see the direct influence of different near-bed orbital wave characteristics on the potential bed-load sediment transport. Ultimately, the potential sediment-transport with currents is calculated, to find an answer to what the potential sediment transport on the Dutch shoreface really is.

6.3.1. Sensitivity analysis: Direct influence of parameters on bed-load sediment transport

The influence of skewness and significant forward orbital velocities are calculated in a sensitivity analysis. The bed-load transport formulations by Van Rijn (2007) use some parameters as input for the bed-load calculation which aren't wave dependent as well, such as sediment grain size diameter D10, D50, D90 in meters, water depth in meters and East and North-oriented current U_r and V_r in m/s. Varying one of these parameters leads to insight in what sediment transport rates could be expected with certain sediment diameters, water heights and currents.

6.3.2. Sensitivity analysis: Indirect influence of parameters on bed-load sediment transport

Via the parameterizations, significant wave height and peak wave period have influence on bed-load sediment transport rates. Information about this influence give insight in the usability of the parameterizations in bed-load sediment transport calculations.

6.3.3. Weighting and comparison of found orbital wave characteristics and potential sediment transport rates

The previously mentioned methods are used to find the orbital wave motion characteristics forward orbital velocity, skewness and asymmetry. Also, the potential bed-load sediment transport is determined. Table 4 illustrates the fact that both ADV's sometimes generate data on different moments and contain data gaps, and that the transformation matrix generates data each three hour. Orbital velocities, skewness, asymmetry and sediment transports must be compared between the parameterizations and the measured velocity signals with the ADV's. The parameterizations depend on the Transformation matrix. Row A & B in Table 4 illustrate on which moments the transformation matrix and ADV's could be compared. Outcomes of the parameterizations and the measured velocity signals must be compared between the two measurement frames. This is only possible for the moments in row C.

Hs-values from Transformation matrix for frame 1														
Hs-values from Transformation matrix for frame 3														
High ADV frame 1 generates data														
High ADV frame 3 generates data														
Time in minutes	0	30	60	90	120	150	180	210	240	270	300	330	360	390
A) Hs-values during ADV-data frame 1														
B) Hs-values during ADV-data frame 3														
C) Hs-values during ADV-data frames 1 & 3														
D) Hs-values during ADV-data frame 1 or 3														

Data available	
Data not available	

Table 4 – Schematic representation of options for comparison parameterizations and measured velocities over time

When comparing the research outcomes of frame 1 with the research outcomes of frame 3, a small data set is left over in row C. Furthermore, the data generated with the ADV's is collected during the autumn. During autumns, considerably more storms occur than during year-round conditions. To compare found asymmetry's, skewnesses, sediment transports etc. between the two measurement frames and with year-round conditions, weight-averaging is needed.
The used transformation matrix data set contains data from 1 January 2013 till 31 December 2017, so it contains year-round conditions. Figure 24 shows the cumulative relative frequencies of the significant wave height for year-round conditions and the significant wave height during measured ADV-data.

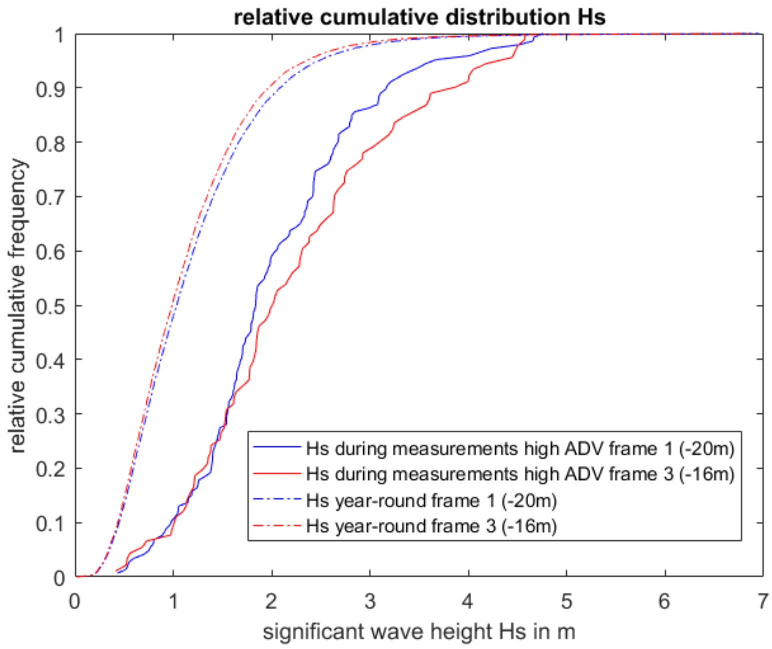

Figure 24 - Cumulative relative distribution Hs during period in which one of the ADV's is active, and during 2013-2017

The higher the significant wave height, the higher the wave energy, so the higher the bed-load sediment transport. Figure 24 shows that during measured ADV-data, the significant wave heights were higher than significant wave heights over the period between 2013-2017. The Hs-values of the entire 2013-2017 time series for frame 3 are lower than those for frame 1. For Hs-values during the ADV-measured time periods, the Hs-values for frame 3 are higher than those for frame 1.
The expected potential bed-load sediment transport on the Dutch lower shoreface for year-round conditions is lower than the expected potential bed-load sediment transport during the measured ADV-bursts, especially for frame 3. Therefore, weight-averaging is applied.
Two weight averages are determined:

- Autumn '17: Weighted averaging for the moments in which one of the high ADV's of Frame 1 or Frame 3 generates data (row D in Table 4) to compare orbital velocity, skewness and asymmetry between both measurement frames.
- Year-round: Weighted averaging for year-round conditions to determine the weighted mean potential bed-load sediment transport rate representative for year-round conditions.

First, Hs-classes are determined for ΔHs=0.5m. The highest class covers the highest 0.5m Hs-values during the ADV-bursts. For the entire Hs-time-series between 2013 and 2017, extreme significant wave heights exist that are higher than those measured during the measurement campaign. These extreme significant wave heights are added to the highest class.

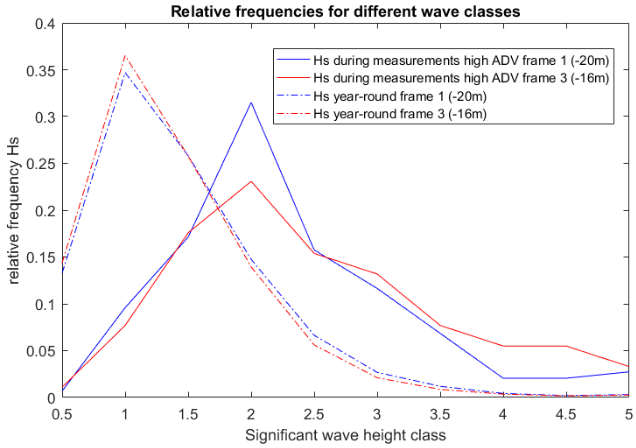

Figure 25 - Relative frequencies of wave classes, the relative frequency is shown at the right-hand side of each bin (e.g. the relative frequency of significant wave heights for frame 1 during 2013-2018 between 0.5 and 1 m is 34,8%. Significant wave heights higher than 5m are added to class 4.5-5m

Calculated or measured Orbital velocities, skewnesses and sediment-transports are grouped per wave class and averaged using the relative frequencies of the Hs-classes during the time in which one of the two high ADV's is active as weights to find values that could be used to compare conditions at -20m NAP and -16m NAP (See Figure 25). The relative frequencies of correspond with year-round conditions. The relative frequencies of the entire transformation matrix data-set are used as weightings to find bed-load sediment transports representative for year-round conditions.

7. Results

This chapter first discusses the effect of different parameters on the orbital wave velocities, skewnesses and asymmetries. Then, the orbital wave velocities and skewnesses of both the calculated orbital wave profiles with parameterizations and the measured velocity signals are discussed and compared.
The effects of currents, sediment grain size, water depth, orbital velocities and skewness on bed-load sediment transport are discussed, before the bed-load sediment transport rates for both calculated orbital wave profiles with parameterizations and measured velocity profiles. The outcomes of these different bed-load sediment transport rates are compared for year-round conditions. At last, a start is made in extrapolating found sediment-transport rates to the entire Dutch coast.

7.1. ADV-data processing results

7.1.1. Wave period

The plots in Figure 26 show the measured mean wave periods with the high and low ADV's on both used measurement frames, as well as the peak wave periods from the transformation matrix at the location of both measurement frames during autumn 2017.

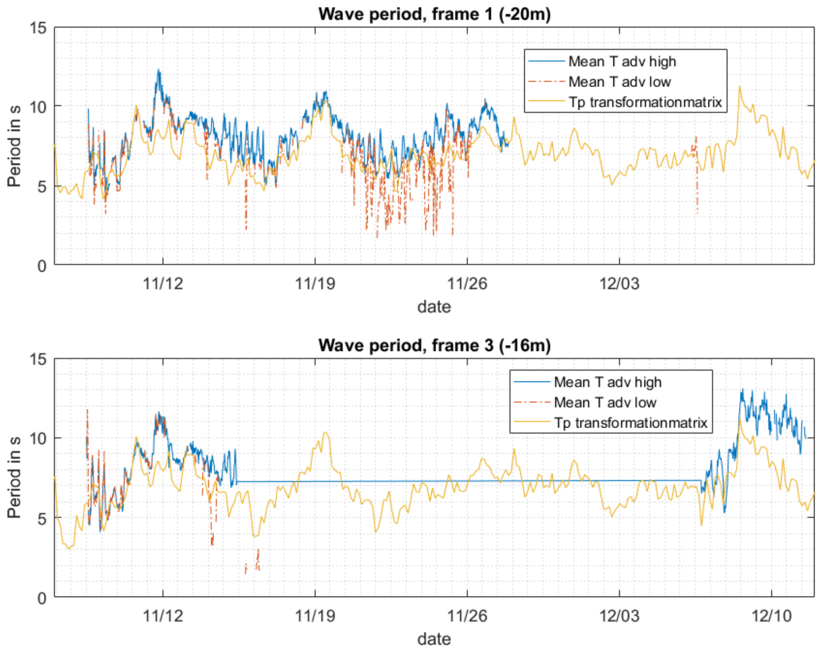

Figure 26 - Wave period during autumn 2017

The low adv's show a large amount of relatively low outliers. The mean wave period measured with the ADV's and extracted from the velocity signal by the WAFO-tools is slightly higher than the peak wave period from the transformation matrix, especially around 10 December 2017 for frame 3. This has two reasons. First, the peak wave period Tp is constructed from wave spectrum analysis, and second, this might be caused by underestimating the amount of zero-upcrossing in the velocity signal due to using a moving average. The highest measured wave periods are about 12 seconds.

7.1.2. Tidal currents

This paragraph deals with the influence of measured current and wave velocities, to see if the expected sensitivity of bed-load sediment transport to different parameters is also true when implementing the measured current and wave orbital velocities or the measured currents are showed in the figure below. Figure 27 shows that the lower ADV's on both measurement frames measure smaller wave and tidal current velocities. The current velocity components in East-West directions are higher than those in North-South directions. This is consistent with the tidal currents on the Dutch coast near the Wadden Islands.

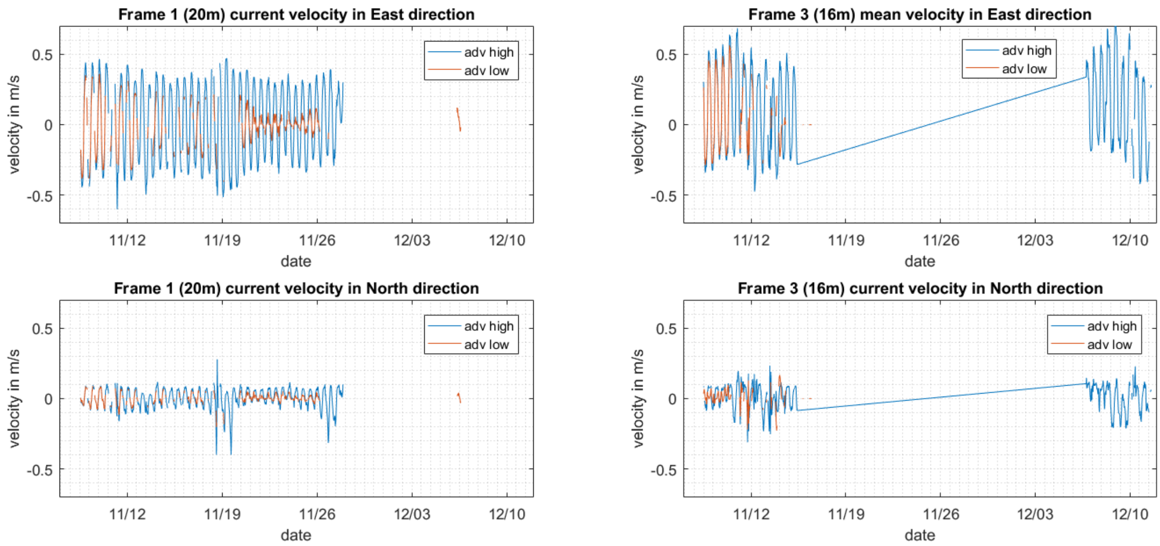

Figure 27 - Current velocities in East and North direction

7.1.3. Orbital motion and tidal current directions

Figure 28 shows the distribution in magnitude and direction of the measured current and wave velocities, for both the high and low ADV's. The average wave direction for frame 1 is approximately 340°, whereas this is 330° for Frame 3. This difference might be caused by the bathymetry of the Amelander Zeegat and its ebb-tidal delta. The magnitude of the tidal current in ebb- and flood direction for frame 1 is almost the same. The ebb-current (80°) at frame 3 is smaller than the flood-current (260°). From this Figure, it might be expected that bed-load sediment at frame 1 is transported in more southern direction than eastern direction, and that the bed-load sediment at frame 3 is transported slightly more in East and less in South direction.

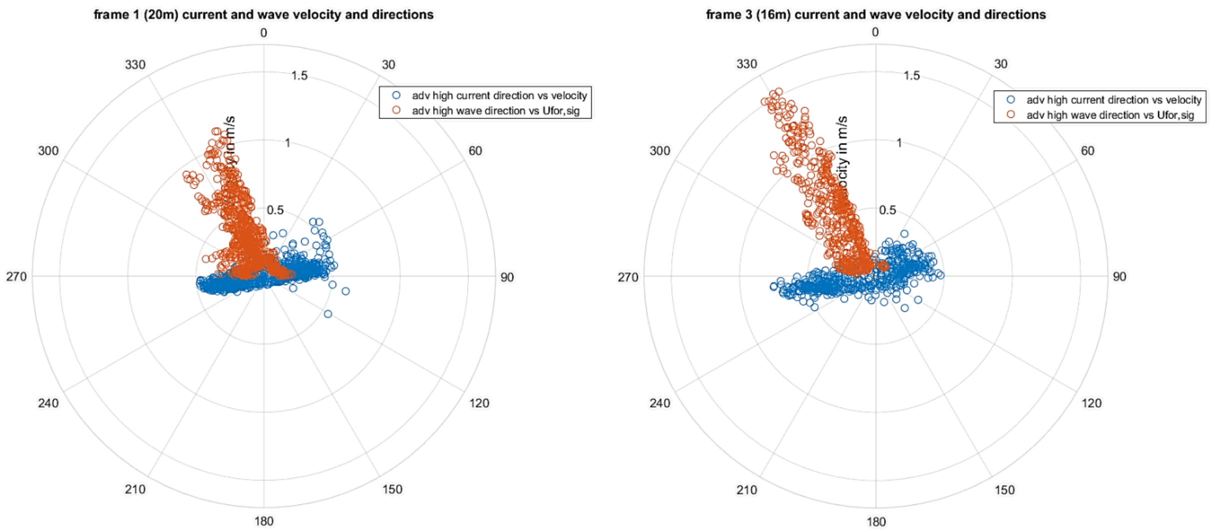

Figure 28 - Current and wave directions. Each dot represents the mean velocity magnitude and direction per 30min.

As Figure 29 shows, the wave directions from the adv's are relatively more southward directed than the wave directions from the transformation matrix, especially for the measurement frames. This might be because of bathymetric effects. The ADV's are near bed, near-bed velocity is influenced by the shape of the bed. The transformation matrix does not take bathymetry into account.

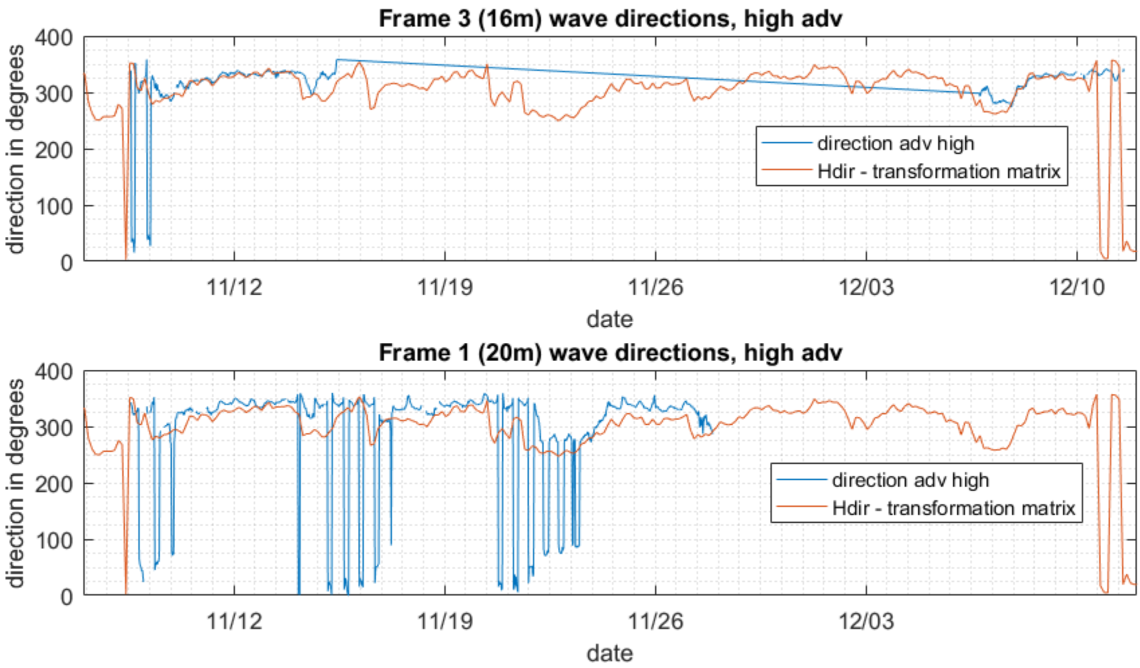

Figure 29 - Wave directions, comparison for transformation matrix and near-bed wave directions

7.2. Near-bed orbital wave characteristics

The influence of parameters on near-bed orbital wave characteristics is determined in sensitivity analysis. Afterwards, the measured and calculated near-bed orbital wave characteristics with parameterizations are compared.

7.2.1. Sensitivity analysis: Influence of parameters in parameterizations on near-bed orbital wave characteristics

In this paragraph, the role of the parameters water depth, significant wave height and peak wave period in the parameterizations of Isobe & Horikawa (1982) and Ruessink et al. (2012) is discussed. This is done by varying one parameter while keeping other parameters constant.

As input for the variables which are kept constant, the values in Table 5 are used. These values are realistic for the water depths and circumstances at the locations of the measurement frames. All constant parameters are pragmatically chosen in such a way that varying the other parameters show patterns in the calculated forward significant orbital velocity, skewness and asymmetry for relatively energetic waves.

	Min	Max	Constant
Hs (m)	0	5	3,5
Tp (s)	2	13	11

Table 5 – Lower limit and upper limit for varying parameters, and value if kept constant

Water depth

Waves approaching the shore become more skewed as the water depth decreases. In Figure 30, the waveshape at heights 16 and 20m are shown, with values in Table 6.

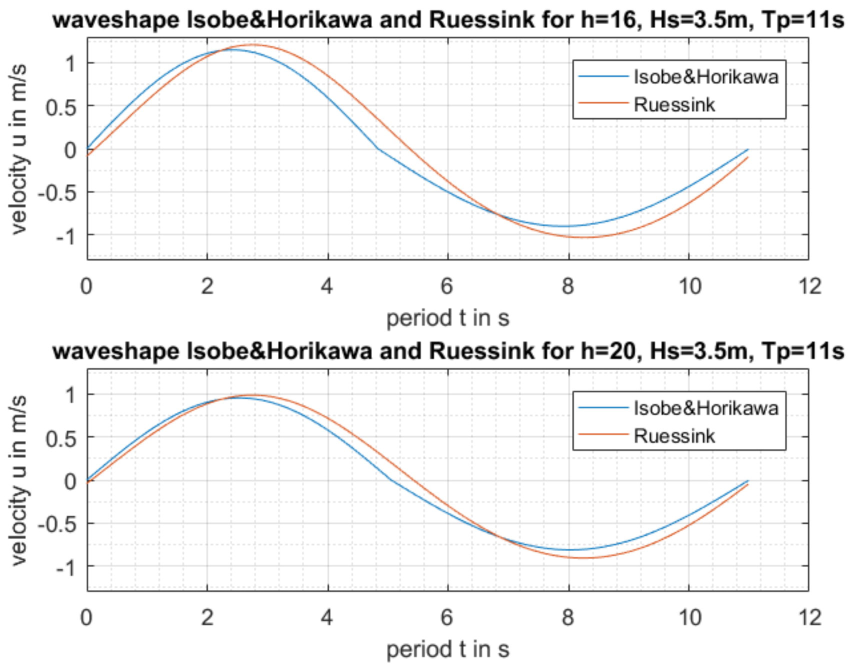

Figure 30 - waveshape Isobe-Horikawa & Ruessink for h=16m & h=20m

Depth	16m	20m
$U_{for,IH}$ (m/s)	1,15	0,96
$U_{for,AR}$ (m/s)	1,21	0,99
$R_{u,IH}$ (-)	0,56	0,54
$R_{u,AR}$ (-)	0,54	0,52
β_{AR} (-)	0,50	0,50

Table 6 – Near-bed orbital wave characteristics for the waveshapes in Figure 28

At both depths, the asymmetry β for the Ruessink parameterization is 0,50, which means the waveshape for both depths is symmetric. The forward orbital velocity calculated with the Ruessink parameterization is higher than the one calculated with the Isobe-Horikawa parameterization. The difference between the forward orbital velocity of both parameterizations decreases as the depth increases. Although the Isobe&Horikawa-parameterization gives smaller forward orbital velocities, it gives a more skewed velocity signal than the Ruessink parameterization at both water heights. The Isobe&Horikawa-parameterization shows a discontinuity in the velocity profile at both depth.

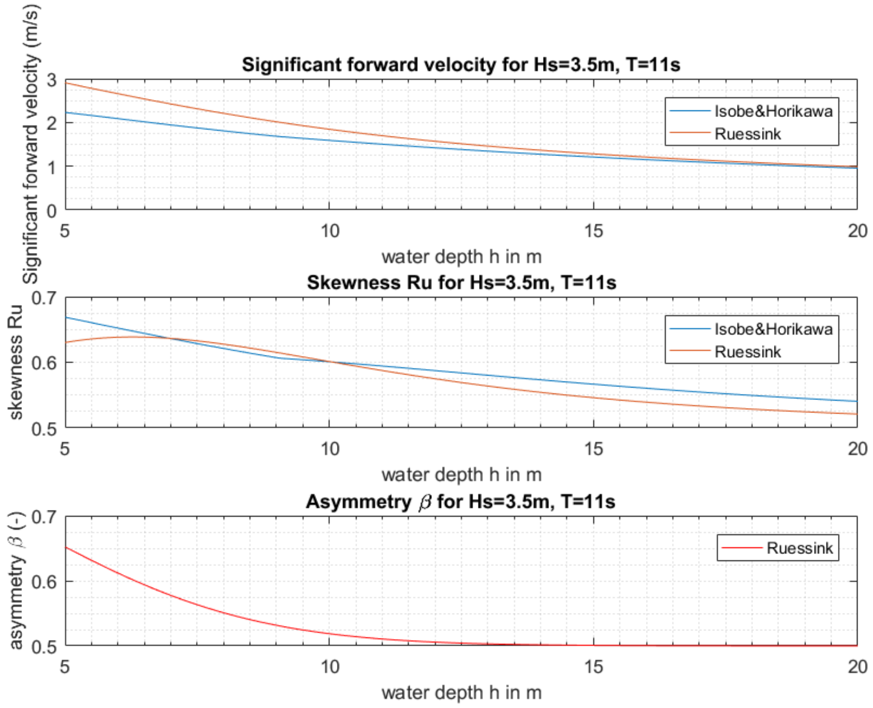

Figure 31 – Significant forward orbital velocities, skewness Ru and asymmetry β for different water depths

Figure 31 shows the forward peak velocity, skewness R_u, asymmetry β and the sediment transport in m^3/y/m for the height profile between 5 and 20m below NAP. For a depth of 5m, the forward peak velocity for Hs=3,5m and Tp=11s is almost 3,5 m/s calculated with the Ruessink-parameterization and about 2,1 m/s for the Isobe&Horikawa-parameterization. The velocities decrease to about 1,9 m/s and 1,8 m/s at 10m water depth respectively, and further to about 1,2m/s at 15m and 1m/s at 20m water depth. The IH-parameterization show higher forward significant orbital velocities than the Ruessink-parameterization, but this difference decreases with the water depth.

For the given Hs- and Tp-values, both parameterizations show forward skewed waves (Ru>0,5). For water depths larger than 10m, the IH-parameterization calculates waves with a higher skewness than the Ruessink parameterization.

The asymmetry β for the Ruessink-parameterization is approximately 0,65 at a water depth of 5m. This diminishes to 0,5 at a water depth of 15m. The forward and backward orbital acceleration is equally large for water depths deeper than 15m. For this reason, asymmetry is not involved in further sensitivity analysis.

Significant wave height
Figure 31 shows the influence of the significant wave height on forward peak velocity, skewness and sediment transport without current for water depths of 16 and 20m respectively.

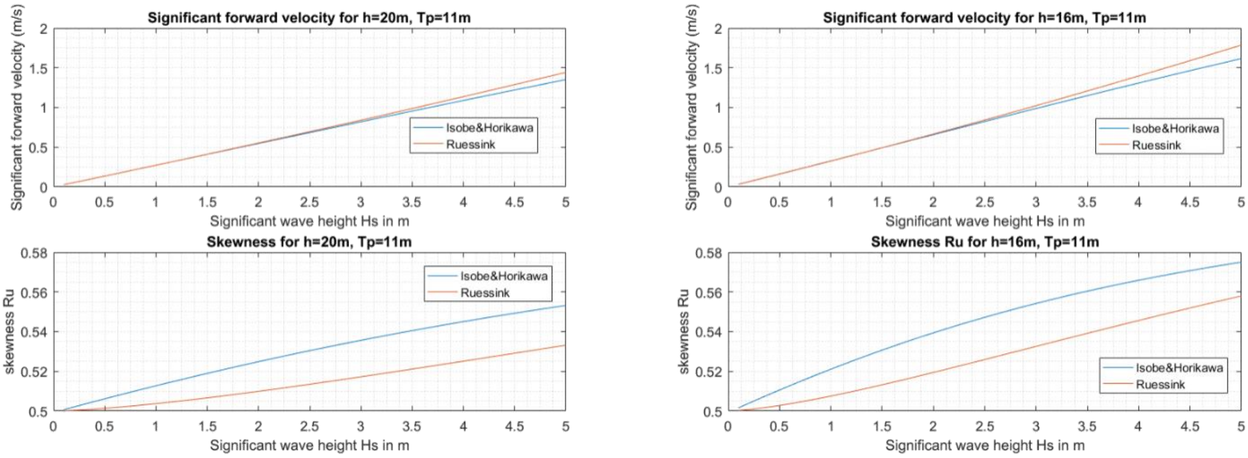

Figure 32 – Influence of significant wave height on forward peak velocity and skewness Ru

For both water depths, the forward significant orbital velocity calculated with the Ruessink-parameterisation is higher than the IH-parameterization. The forward significant orbital velocities at -16m NAP are about 1,8 m/s and 1,6 m/s and 1,4 m/s and 1,3 m/s at -20m NAP for the Ruessink- and Isobe&Horikawa-parameterizations respectively. At larger water depths, the difference in velocity between both parameterizations becomes larger. Both parameterizations show an almost linear relation between significant wave height and forward peak velocity.
The skewness for both parameterizations without surface waves is 0 for all water depths. At -16m the skewness Ru increases to 0,58 for the IH-parameterization and 0,56 for the Ruessink-parameterization at a significant wave height of 5m. At -20m, the skewness Ru increases to 0,56 for the IH-parameterization and 0,53 for the Ruessink-parameterization at a significant wave height of 5m.
Significant wave height has a smaller effect on the forward orbital velocity and skewness for a larger water depth.

Peak wave period

Figure 33 shows that the peak wave period higher than a certain threshold value have impact on the calculated forward orbital velocities and skewnesses for both parameterizations.

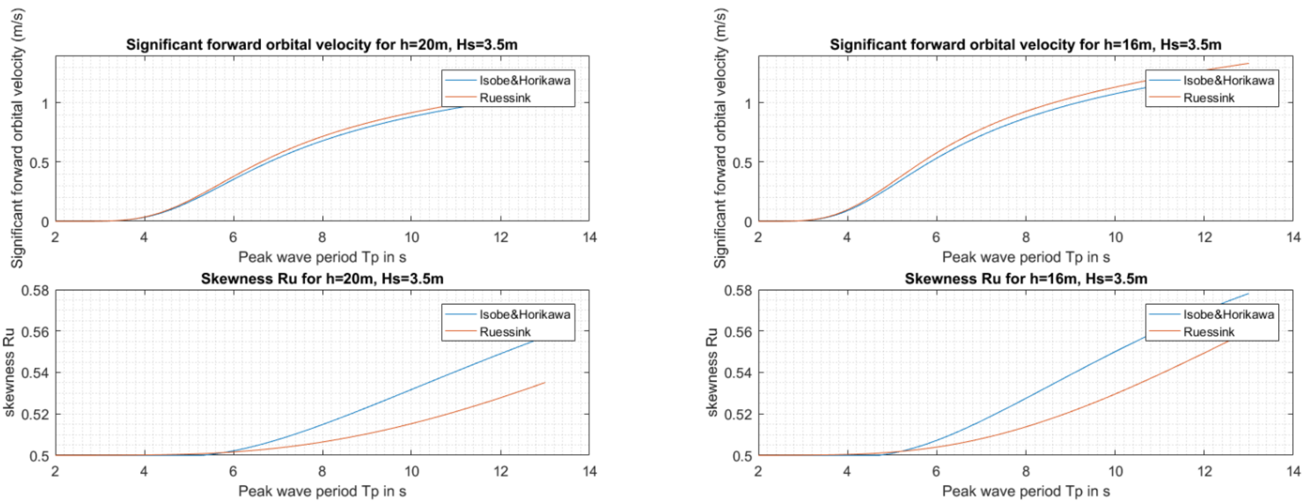

Figure 33 – Influence of peak wave period on significant forward orbital velocity and skewness Ru

For the forward orbital velocity, this threshold value lies at a peak wave period of 3s for -16m NAP, and 3,5s for -20m. The Ruessink velocity profile shows slightly higher forward orbital velocities than the Isobe-Horikawa parameterization. For -16m NAP, the forward orbital velocity increases to about

1,3m/s for both parameterizations at a peak wave period of 13 seconds. For -20m NAP, a peak wave period of 13 seconds yields a forward orbital velocity of 1,1m/s for the parameterizations.

For the skewness Ru, this threshold value lies at a peak wave period of approximately 4s for -16m NAP, and 5,5s for -20m. After reaching the threshold value, the skewness Ru increases faster for the Isobe&Horikawa parameterization than for the Ruessink-parameterization. For -16m NAP, the skewness increases to about 0,58 for the IH-parameterization and 0,56 for the Ruessink-parameterization at a peak wave period of 13 seconds. For -20m NAP, a peak wave period of 13 seconds yields a skewness of about 0,56 for the IH-parameterization and 0,53 for the Ruessink-parameterization.

The peak wave period has a smaller effect on the forward orbital velocity and skewness at 20m than at 16m water depth.

7.2.2. Sensitivity Analysis: sub-conclusion

The Isobe&Horikawa parameterizations predict waves with a higher skewness than the Ruessink-parameterization. The Ruessink-parameterization predicts larger orbital velocities than the Isobe-Horikawa parameterization. Forward orbital velocity, skewness and asymmetry decreases as the water depth increases. At water depths larger than 15m, the predicted waves with both parameterizations are completely symmetric. Significant wave height has a larger influence on forward orbital velocity.

7.2.3. Comparison of near-bed orbital wave characteristics

The Forward orbital velocity, skewness, asymmetry and skewnesses could be compared, both over time, as well as relative to the significant wave height.

Orbital velocity

The forward peak velocities measured from the ADV's are plotted in Figure 34 and compared to the forward orbital velocities calculated with the Ruessink and Isobe-Horikawa parameterizations.

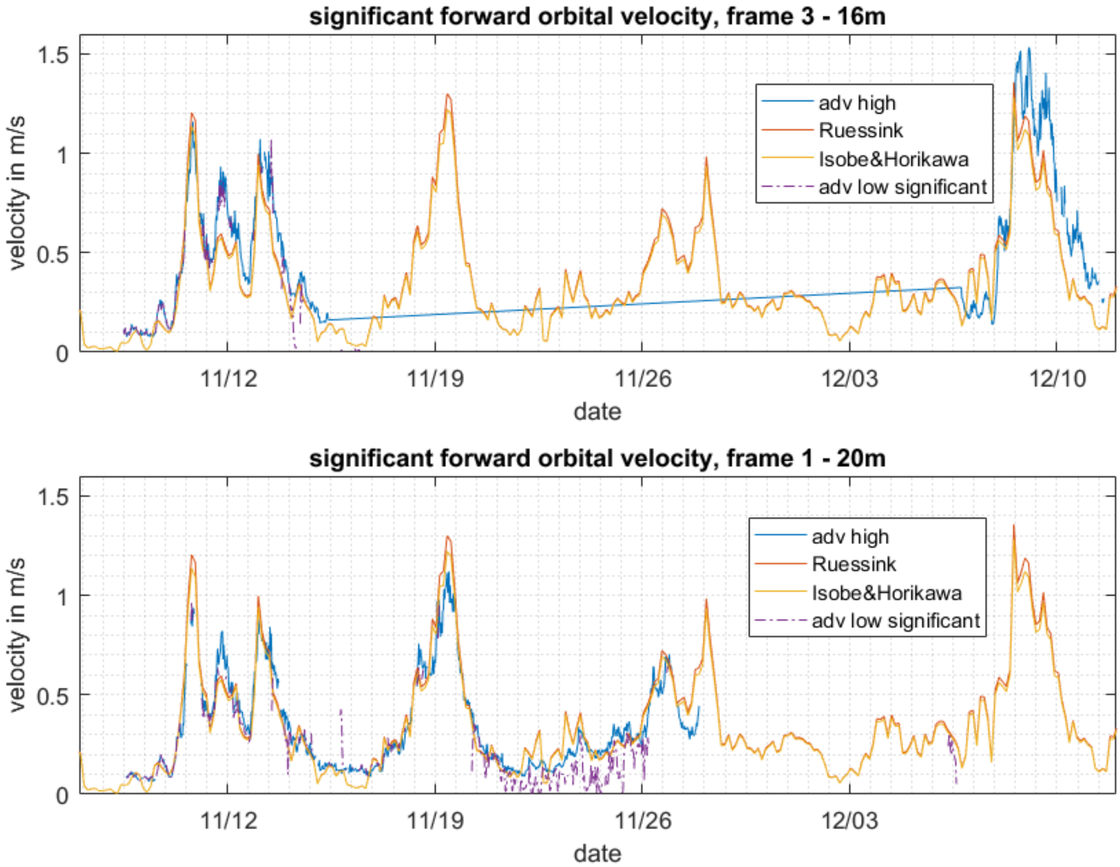

Figure 34 – Significant forward orbital velocity for measurement series

The upper ADV shows higher forward orbital velocities than the lower due to bed shear stress. It is clear from Figure 34 that the lower ADV does not produce data when the forward orbital velocities rise at peak events, such as the peak on 19 November 2017. This is troublesome for determining sediment transports later in this research, because sediment-transports are exponentially related to forward velocity, from a certain forward velocity, bed-load sediment is transported substantially. In this research, bed-load sediment transports will be calculated with the high adv's only.
The fact that the Ruessink parameterization gives slightly higher forward orbital velocities than the Isobe-Horikawa parameterization is also in line with the findings from paragraph 7.2.1, especially at peak energy events.

The maximum reached significant forward orbital velocities during autumn 2017 are about 1,3m/s at -20m NAP and 1,5m/s at -16m NAP.

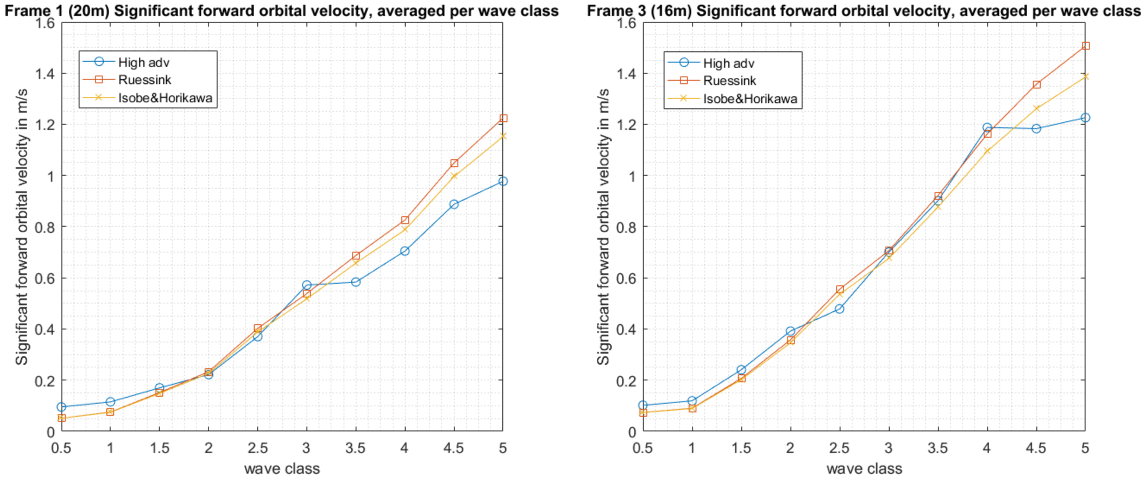

Figure 35 – mean significant orbital velocity per wave class

In Figure 35, the significant forward orbital velocity is plotted against the significant wave height classes. The difference in significant orbital velocity between the Isobe-Horikawa and Ruessink parameterizations increases as the waves become higher. The Ruessink-parameterization gives slightly higher significant forward orbital velocities than the IH-parameterization. The mean orbital velocities of the Parameterizations resemble quite well with the measured orbital velocities, as could be seen in table 7.

Mean	Frame 1	Frame 3
Measured	0,34	0,55
Ruessink	0,35	0,56
IH	0,34	0,54

Table 7 - Mean skewnesses

The orbital velocities for both frames could be compared when applying weighted averages for the time intervals in which the high ADV's on both frames are active. This is important, because Figure 34 shows that the high ADV on frame 3 measures relatively much high energy events, compared to the high ADV on frame 1.

Weighted average for period in which at least one of the high ADV's generated data	Frame 1	Frame 3
Measured	0,37	0,50
Ruessink	0,39	0,51
IH	0,38	0,49

Table 8 - Weighted averaged skewness

Table 8 shows that after weighting, the mean significant orbital velocities at -20m NAP are approximately 0,10m/s lower than the mean significant orbital velocities at -16m NAP.

Skewness

With the methods prescribed in chapter 5, the skewness R_u is determined from each burst and plotted in Figure 36. The skewness mostly follows the trend of the skewnesses calculated from the parameterizations. However, negative skewnesses are measured as well, mostly for the lower adv's for data with low orbital motion. Mostly at events with high orbital velocities, waves become skewed, according to the parameterizations.

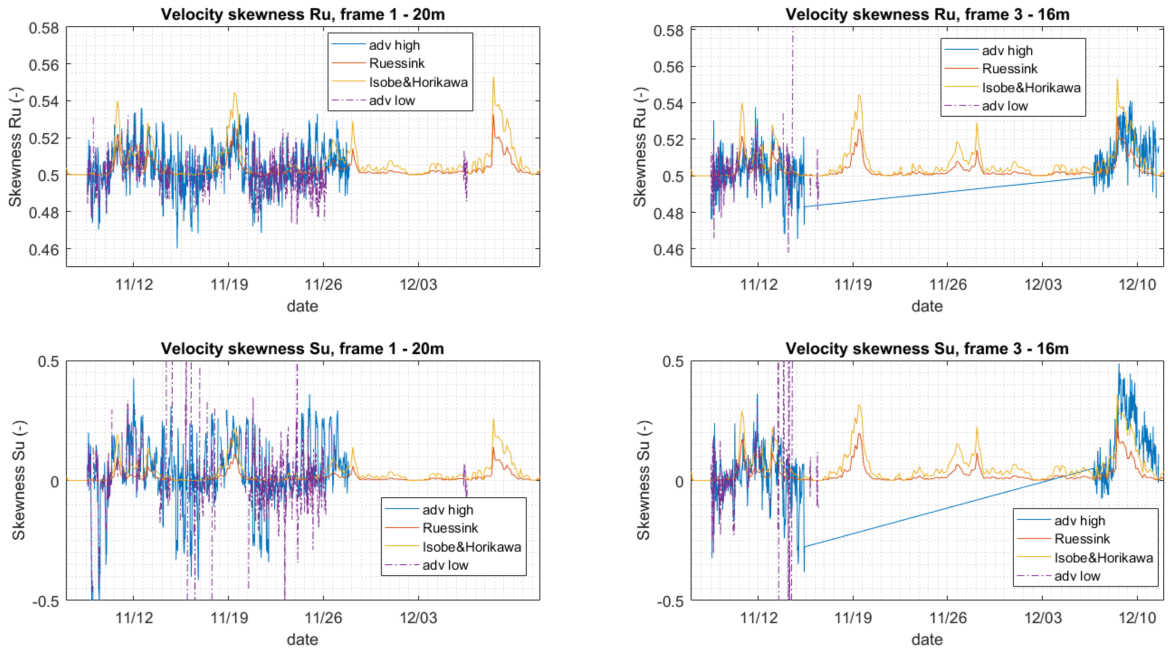

Figure 36 - Skewness Ru and Su for measurement series

Although the skewness for both skewness indicators in Figure 36 show large spikes, a relatively continuous profile is shown when averaging the skewness per wave class and plotting the skewness against the wave class. (Figure 37).

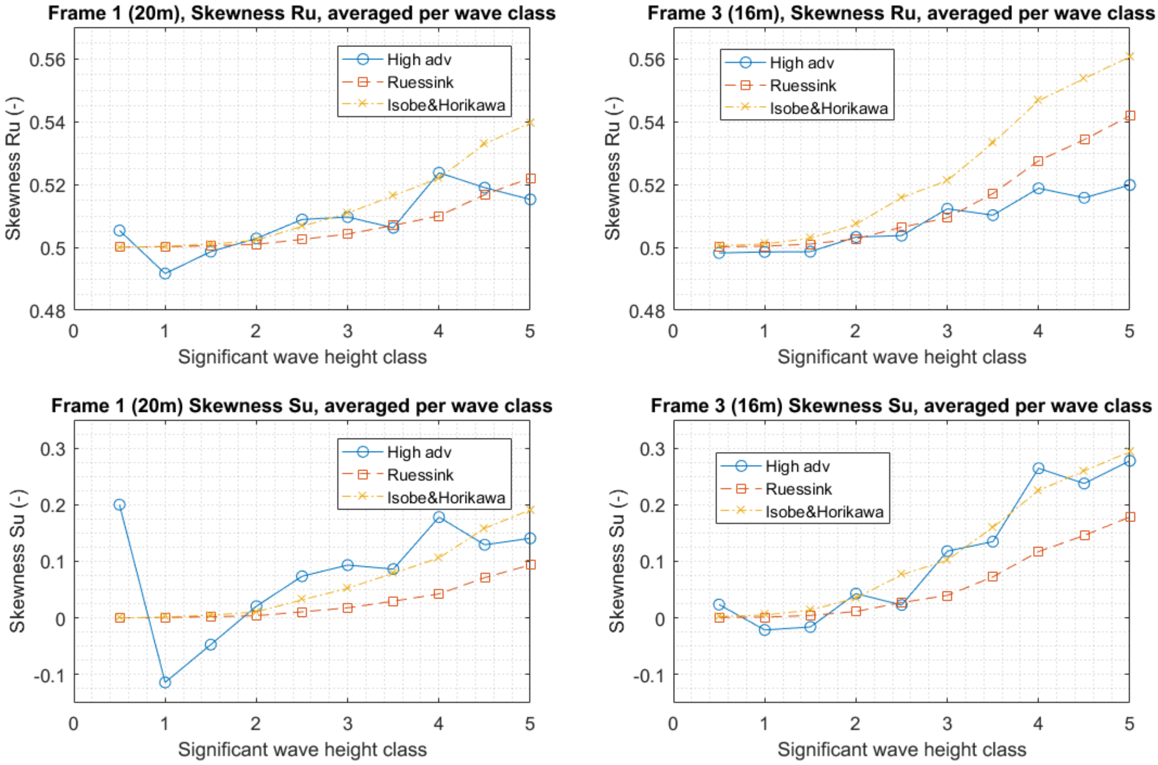

Figure 37 - Skewness per wave height class

Waves between 0,5 and 1,5m show negative skewnesses. The possibility of negative skewnesses was also observed by Ruessink et al. (2012), but not implemented in one of the parameterizations. The Isobe-Horikawa parameterization gives more skewed waves than the Ruessink parameterization. Figure 27 shows that higher waves are accompanied by higher skewnesses.

Mean	Frame 1 (-20m)		Frame 3 (-16m)	
	Ru	Su	Ru	Su
Measured	0,51	0,03	0,50	0,07
Ruessink	0,50	0,01	0,51	0,04
IH	0,51	0,03	0,52	0,08

Table 9 – mean skewness

Although the IH-parameterization does not include negative skewness, the IH-parameterization shows almost the same mean Ru-skewness as the measured velocity signal. The Ruessink-parameterization underestimates the Ru-skewness. This was also expected from the information in Paragraph 7.2.1

Weighted average for period in which adv's on both frames are active	Frame 1 (-20m)		Frame 3 (-16m)	
	Ru	Su	Ru	Su
Measured	0,51	0,04	0,50	0,06
Ruessink	0,50	0,02	0,51	0,03
IH	0,51	0,04	0,52	0,07

Table 10 – weighted skewness

Table 10 shows that, as expected from the sensitivity analysis in paragraph 7.2.1, the waves at -20m NAP are less skewed than those at -16m NAP, when looking at the Su skewness indicator.
It is important to be careful in analysing these results, the correlation between depth and skewness is not so clear when looking at the Ru indicator. The Su-indicator could be more reliable, as it uses an entire time series as input, instead of only the significant forward- and backward orbital velocities.

Asymmetry

In Figure 38, The asymmetry parameters β and Au are plotted. As mentioned before, the β-parameter does not apply for the Isobe-Horikawa parameterizations. Looking at both parameters, the asymmetry-values from the parameterizations is almost equal to 0.5 (β), and 0.0 (Au). There are spikes in the data. The trend for β for frame 3 is slightly higher than for frame 1, which was to be expected. The Au for frame 1 is slightly positive, which describes backward leaning waves. The Au for frame 3 is slightly positive, for forward leaning waves, but it is hard to make conclusions from these small differences. Looking at another dataset displayed in Figure 39, it might even be negligible.

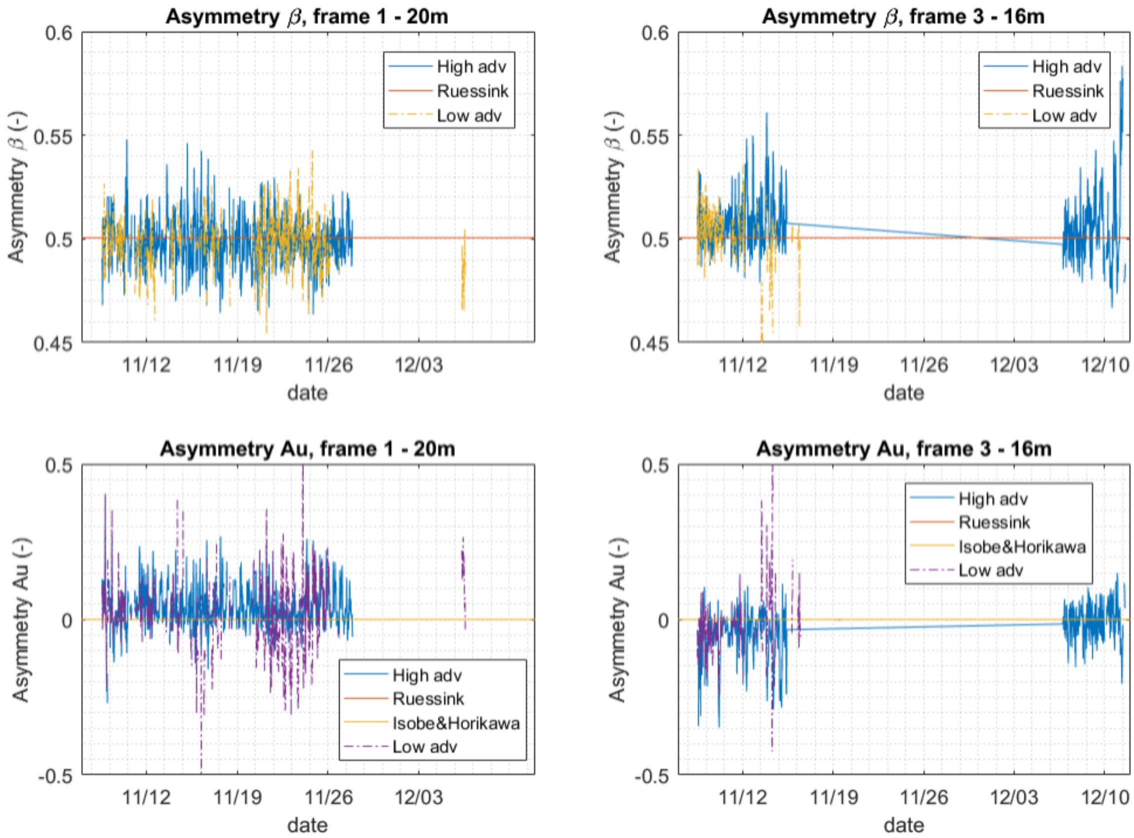

Figure 38 - Asymmetry β and Au

In Figure 39, the measured Au and Su asymmetries and skewnesses are added to the plot of Ruessink et al. (2012) in which skewness and asymmetry is plotted against the Ursell-number, shown in figure 6. The samples used by Ruessink et al. (2012) are taken at another location, with smaller water depth. A higher water depth leads to a higher Ursell-number, therefore the measurement frame samples are located on the left side of the figure. The data from the measurement frames show less negative skewnesses than the dataset used by Ruessink et al. (2012). The fit of the data in Figure 3 is an indicator that the Au and Su parameters are valid parameters in this research

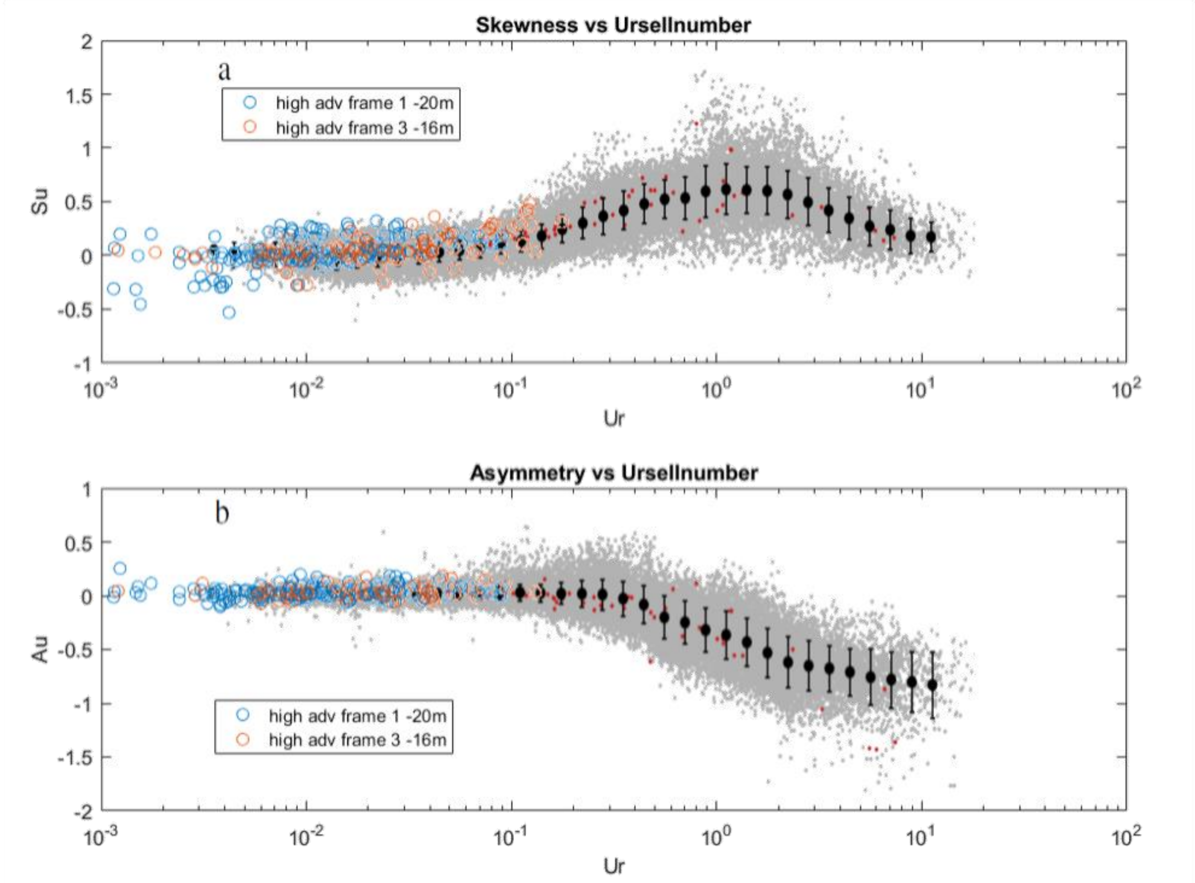

Figure 39 - Ursellnumber vs asymmetry and skewness

7.3. Potential bed-load sediment transport

The influence of direct and indirect parameters on potential bed-load sediment transport, calculated with the Van Rijn (2007) formulations is determined and the transport rates calculated from parameterizations and measured velocity signals are compared.

7.3.1. Sensitivity analysis: Direct influence of wave orbital characteristics on bed-load sediment transport

Orbital velocities and skewness

It is important get insight in the direct influence of significant forward orbital velocity and skewness on bed-load sediment transport. For the skewness, the parameter Ru is chosen, as the backward orbital velocity needed in the Van Rijn (2007) calculations is easy to calculate with Equation 1 when the forward orbital velocity and Ru-skewness is known. The minimum, maximum and constant values in Table 11 are pragmatically chosen and realistic for the study area.

	Min	Max	Constant
$U_{for,sig}$ (m/s)	0	2	0,9
Ru (-)	0,46	0,60	0,53

Table 11 - Parameters for influence of orbital velocities and skewness on bed-load sediment transport

Figure 40 shows that the influence of skewness on bed-load sediment transport varies within order size of 50-100m3/y/m. The difference between 16 and 20m water depth is about 20m3/y/m for all different skewness values.

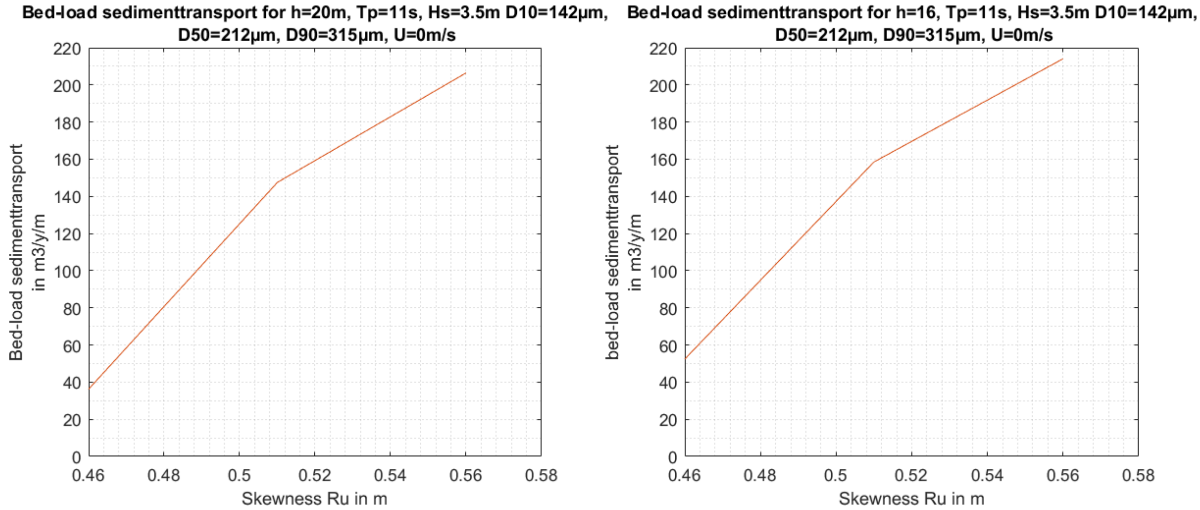

Figure 40 - Influence of skewness on sediment transport

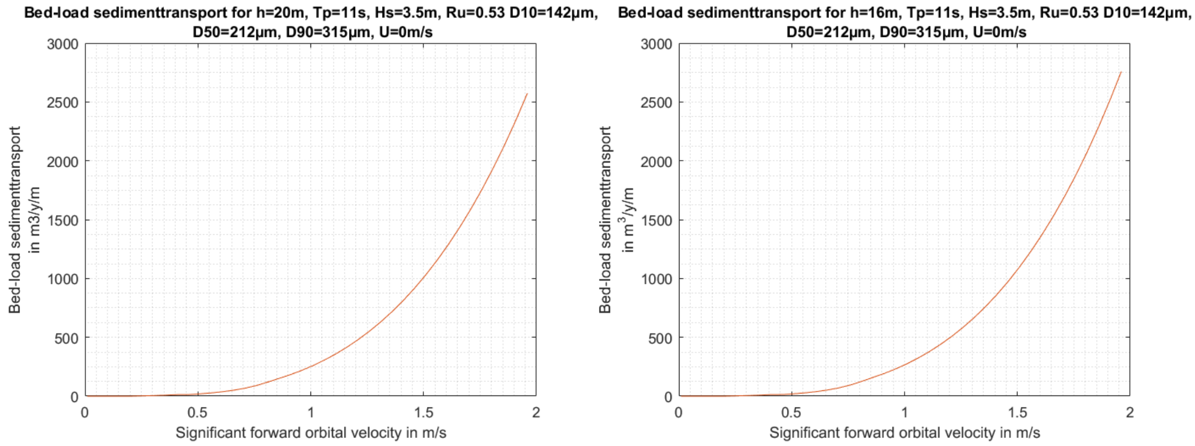

Figure 41 - Influence of significant forward orbital velocity on bed-load sediment transport.

The influence of forward orbital on bed-load sediment transport is much larger (Figure 41) and shows a profile in which higher forward orbital velocities causes much higher sediment-transport rates. The difference between both water depths is about 300m3/y/m for a significant forward orbital velocity of 2m/s. In paragraph 7.2.1 was concluded that the Ruessink-parameterization causes higher forward orbital velocities and lower skewnesses than the Isobe & Horikawa parameterization. Therefore, the bed-load sediment transport rates, calculated with the Ruessink-parameterization as input are higher than the bed-load sediment transport rates, calculated with the Isobe & Horikawa parameterization.

7.3.2. Sensitivity analysis: Direct influence of other parameters on potential bed-load sediment transport

Parameters which don't have influence on the parameterized waveshapes but do have influence on sediment transport are displayed in Table 12. These parameters are used to vary the minimum and maximum sediment grain sizes are the minimum and maximum grain sizes found in samples in the area (see Table 17) The constant values are the mean of samples D28 and D29, near the measurement frames. The minimum current is -0,8 m/s, the maximum current is set on 0,8 m/s, which is a realistic tidal current velocity range. These current velocities are applied in the same direction (or opposite) as the wave direction. As a constant value when varying other parameters, $U_{current}$ is kept at 0 m/s, to find the influence of the other parameters, without current.

	Min	Max	Constant
D10 (μm)	105	165,8	141,8
D50 (μm)	185,9	232,5	211,9
D90 (μm)	288,9	337,2	315,3
$U_{current}$ (m/s)	-0,8	0,8	0

Table 12 – Lower limit and upper limit for varying parameters, and value if kept constant

Influence of current on sediment transport

The maximum current velocity in the current direction measured with a high ADV is about 0,8 m/s. Plotting an increasing current in for h=16m and h=20m shows an increasing sediment transport. The influence of current on sediment transport is stronger at a water depth of 16 meters (See figure 42). The higher the current, the higher the difference in bed-load sediment transport, calculated with both parameterizations. This might be because, as mentioned in paragraph 7.2.1, the Ruessink-parameterization shows higher orbital velocities and the Van Rijn (2007) bed-load transport formulations use a ratio of wave orbital velocity divided by current velocity to determine the apparent bed roughness. The higher the orbital wave motion, the higher the difference between sediment transport calculated with the IH & AR parameterizations. Sediment transport becomes larger at a higher current, it seems that according to the Van Rijn (2007) bed-load transport formulations, waves and current enhance each other when in the same or opposite direction. In Figure 42, the transport for currents perpendicular on the wave direction are remarkably lower than currents in the wave direction. At both -16m NAP and -20m NAP, sediment transport by waves is dominant over sediment transport by currents.

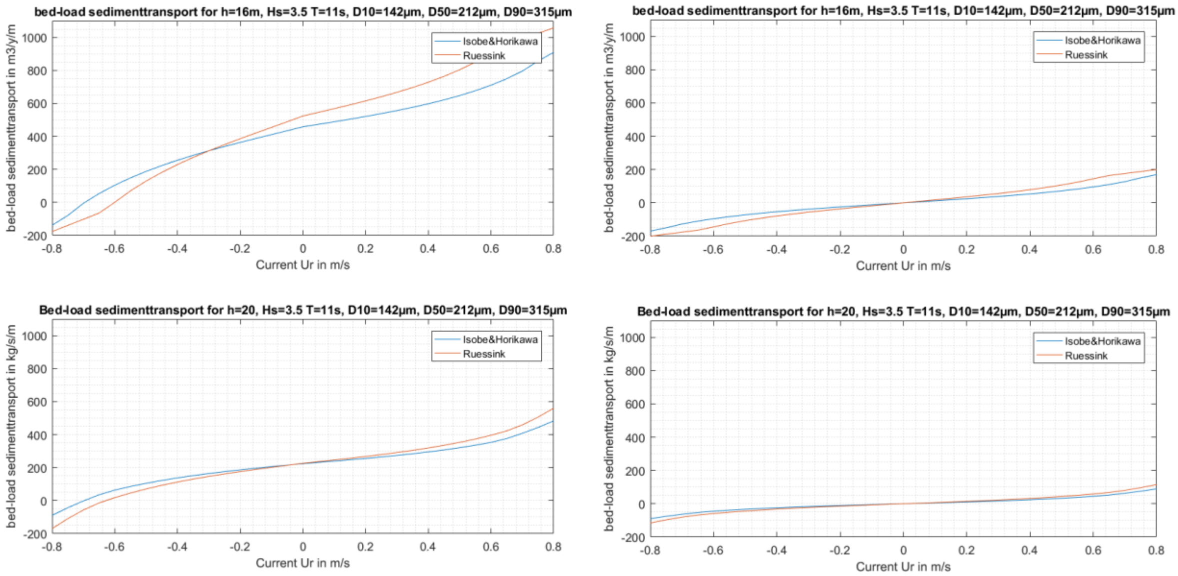

Figure 42 – sediment transport for different current velocities in (left) and perpendicular (right) to the wave direction

Grain size distribution

To find the possible effect of particle size on sediment transport on the lower shoreface near the Amelander Zeegat, the sediment transport is calculated for the minimum, mean and maximum D10, D50 and D90 values for Hs=3,5m, T_p=11s, current U= 0 m/s.

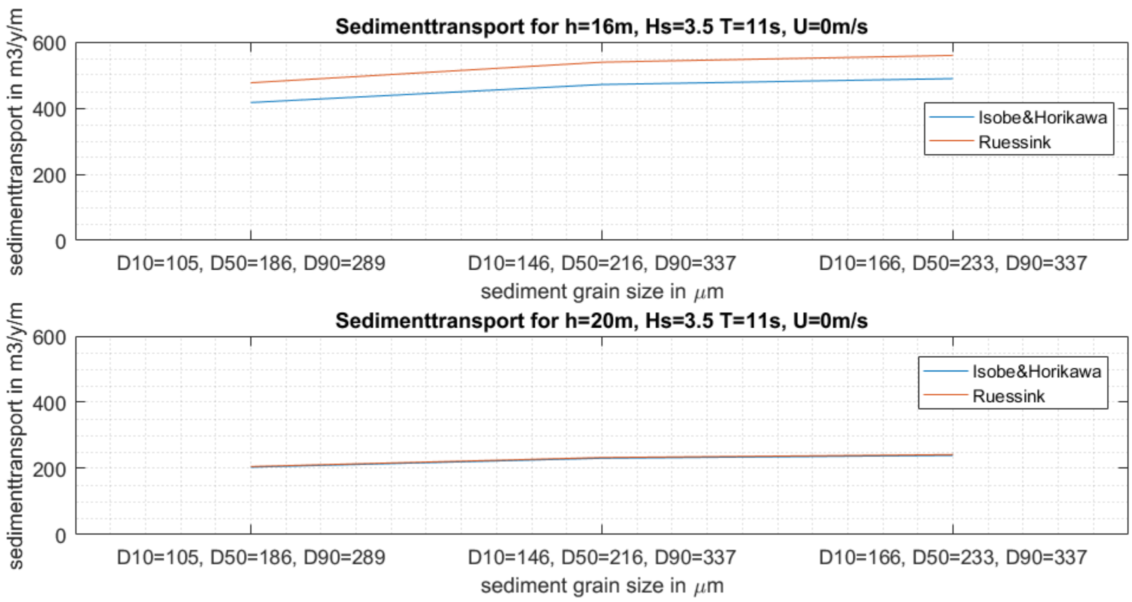

Figure 43 - Effect of particle grain size on sediment transport

Figure 43 shows that the influence of sediment grain size in the range that could be found near the Amelander Zeegat on bed-load sediment transport is low. For -20m NAP, the difference between the smallest and largest grain sizes in the study area is approximately 60m3/y/m, for -16m NAP, the difference is approximately 40m3/y/m.

Van Rijn (2007) shows in Figure 44 the net transport rates measured at Delft Hydraulics as a function of particle size d50=210, 320, and 970 μm, d10=130, 180, 850 μm and d90=180, 320, and 1,200 μm. The current velocity is about 0.25 m/ s at a height of 0.1 m above the bed, the peak orbital velocity is 1.5 m/ s in sinusoidal wave motion with a period of 7.2 s. The bed-load transport is computed with these values as input. The figure shows an increasing bed-load transport for the computed values between D50=210μm and D50=320μm. This might be the explanation why the sediment-bedload transport calculated in this research increases when the particle diameter increases, while the opposite is expected and verified by measurements (See Figure 43).

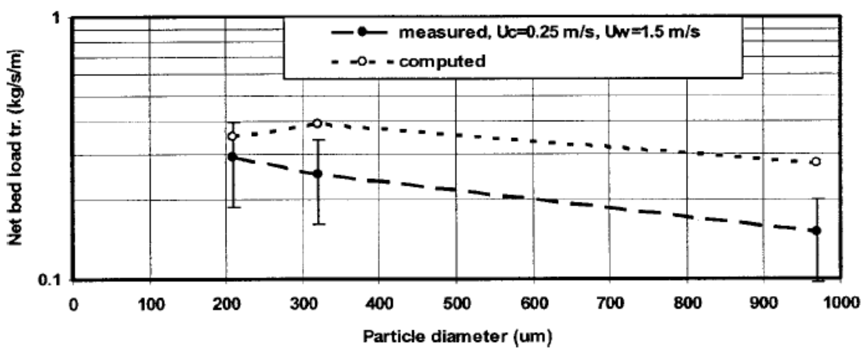

Figure 44 - Net transport in wave boundary layer as function of particle size D50, wave tunnel data of Delft Hydraulics (Van Rijn, 2007)

Water depth

Figure 45 shows the influence on water depth on sediment transport. In shallow water (<10m NAP), the influence of water depth on sediment transport is large. Between 15 and 20m, 5m increase in water depth causes about two third decrease in sediment transport.

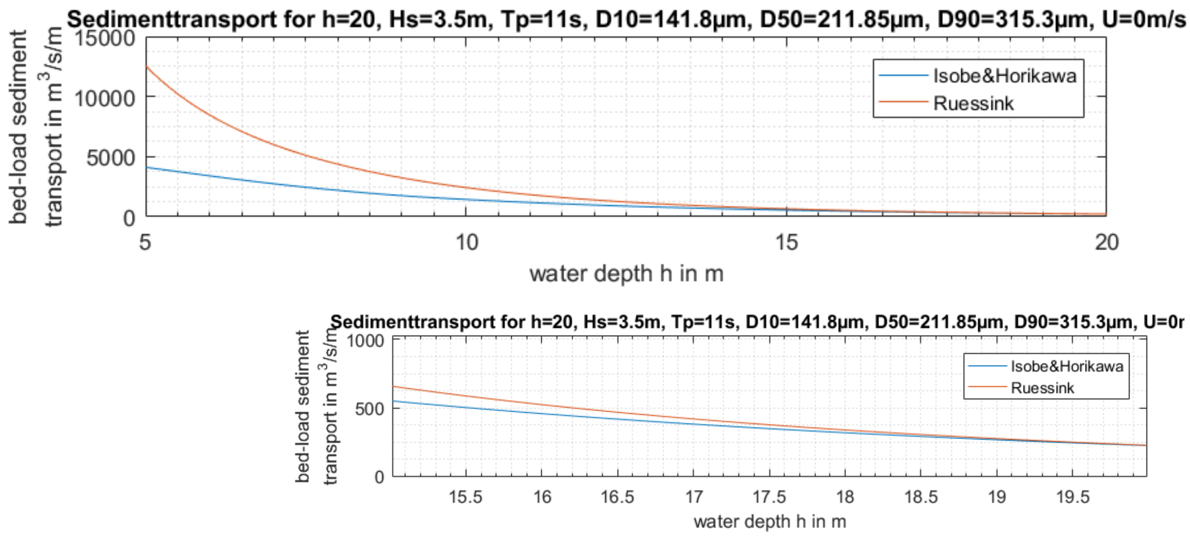

Figure 45 - Influence of water depth on bed-load sediment transport, with detail view for 15-20m

7.3.3. Sensitivity analysis: Indirect influence of parameters on bed-load sediment transport

Peak wave period

Figure 46 shows that the influence of peak wave period on bed-load sediment transport starts at a certain threshold value, different for each water depth (just as the influence of peak wave period on forward orbital velocity (Figure 46). For a water depth of 20m, the increase in sediment transport due to an increasing period is about 400m3/y/m between 8 and 13m. For a water depth of 16m, the increase in sediment transport due to an increasing period is about 200m3/y/m between 8 and 13m. The little bulb at 5,3s (frame 3) and 6s (frame 1) are caused by hard threshold values in the ripple predictor within the Van Rijn (2007) formulations.

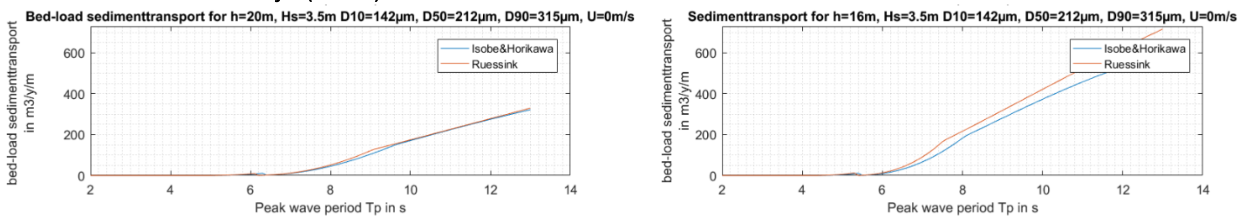

Figure 46 - Influence of peak wave period on sediment transport

Significant wave height

The higher the significant wave height, the more influence it has on bed-load sediment transport (Figure 47). For a water depth of 16m is the increase in sediment-transport between significant wave heights of 2 and 3m approximately 350 m3/y/m, while this increase is 600m^3/y/m between significant wave heights of 3 and 4m for the Ruessink-parameterization. At a water depth of 20m, the significant wave height has a smaller effect: 100m^3/y/m between 2 and 3 meter, and 200m^3/y/m between 3 and 4m for the Ruessink-parameterization.

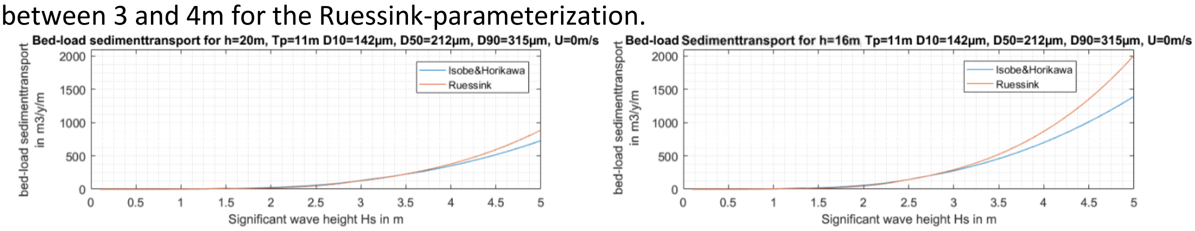

Figure 47 - Influence of significant wave height on sediment transport

7.3.4. Sensitivity Analysis sub-conclusion

When using the Van Rijn (2007) bed-load transport formulations, the bed-load transport rates are most sensitive for forward orbital velocity, followed by peak wave period while the wave period is higher than the threshold value and water depth. Skewness and sediment grain size have the least impact on bed-load sediment transport rates. These sensitivities should be handled with care, the maximum and minimum values for which is the parameters are varied are chosen pragmatically. A choice for other maximum, minimum and constant values might lead to other conclusions.

7.3.5. Comparison of potential near-bed sediment transport rates

As mentioned in paragraph 4.3, the dominant wave direction is North by North West. It could be expected that wave-driven bed-load sediment-transport will be focussed South by South East. In Figure 38 the sediment-transport due to orbital wave motion only (without current) is plotted over time. For the plotted sediment transport, calculated with the parameterizations and with the measured velocity signal, the South by South East-prediction is correct.

A quick look at the data shows that the Ruessink parameterization shows a bit more sediment transport than the Isobe-Horikawa parameterization, in line with the conclusions from the sensitivity analysis. In peak-events, the sediment transport rates for the measured orbital velocities is most of the times lower than the sediment transport rates calculated with the parameterizations. This is because a small difference in forward orbital velocity in high energy events leads to a high difference in sediment transport. The plots show data gaps for the ADV-data. For instance, at the 19 November peak event for frame 3, where there is no data available for the adv's.

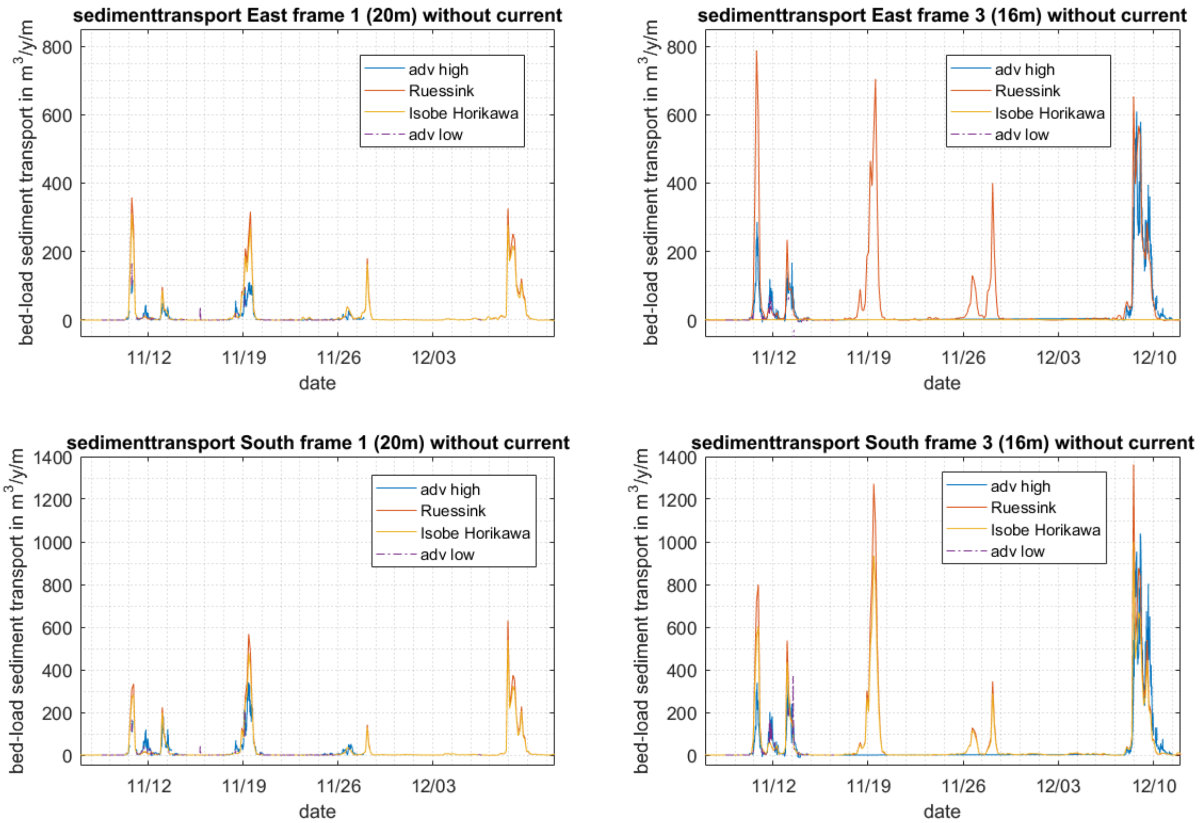

Figure 48 – sediment transport in East and South direction without current

Figure 49 shows the sediment transport with current included in the calculation. Because the current is determined with ADV-data, these plots show less peaks than those without current in Figure 48. The figures show that for low-energy events, for example between 13 and 26 November 2017 for Frame 1, the bed-load sediment transport rates are influenced by tidal currents. Most of the sediment is transported during peak events. This means that the influence of currents on the total amount of transported bed-load sediment is small, the oscillations in Figure 50 show the influence of currents on bed-load sediment transport.

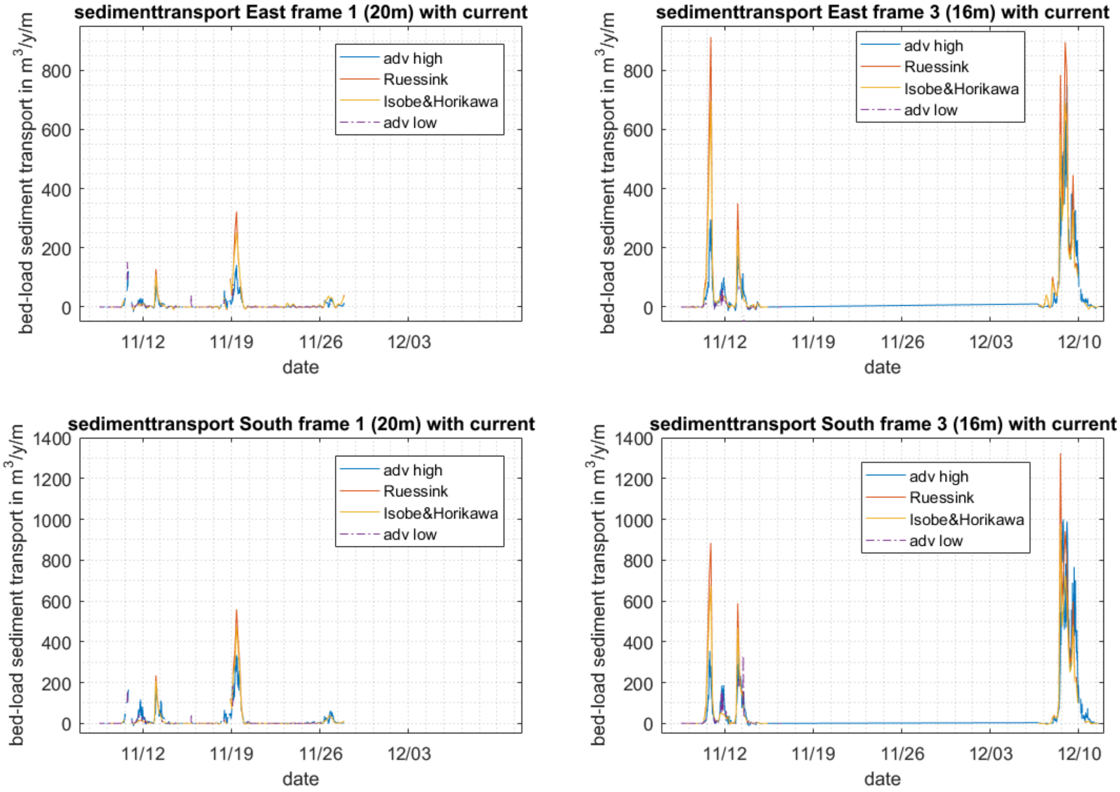

Figure 49 - sediment transport in East and South direction with current

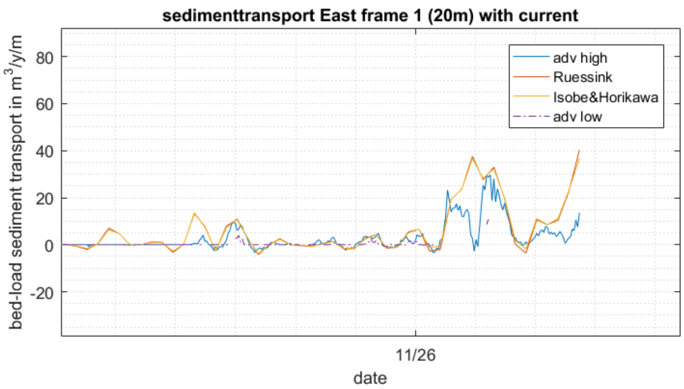

Figure 50 – Detail view on oscillations due to tidal currents

Because the current of the high adv's is applied to calculate sediment transports with the low ADV's, only events at which both high and low adv's generate data are shown in the low adv plots. In the figures below, the potential sediment transport, averaged per wave class is displayed, in cubic meter per year per running meter. The mean and weighted potential sediment transports are listed in Tables 13, 14 and 15. Figure 54 shows higher transports for Frame 3 than for Frame 1, which is in line with the sensitivity analysis. The sensitivity analysis showed that currents enhance sediment transports. The small dip at wave height class 4-4,5m for the sediment transports calculated with measured velocities is due to a small number of samples in that wave-height class. The higher the significant wave heights, the higher the exaggeration of sediment transport rates compared with the sediment transport rates calculated with measured velocities.

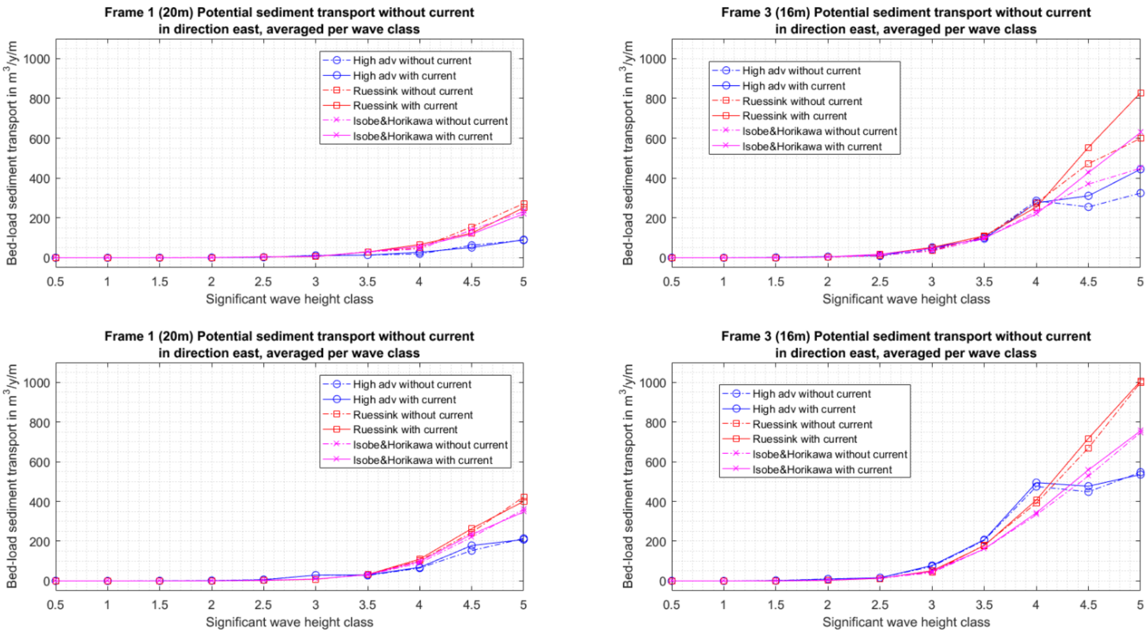

Figure 51 - potential sediment transport without and with current

Tables 13, 14 and 15 show the calculated bed-load sediment transport rates and their directions. Table 13 shows mean transport rates and directions. Table 14 shows the transport rates and directions, weighted averaged over the entire period in which one of the high ADV's is active, to compare data for both water depths. Table 15 shows the transport rates and directions, weighted averaged for year-round conditions.

Mean		Frame 1 (-20m NAP)		Frame 3 (-16m NAP)	
		Transport rate in $m^3/y/m$	Direction in °	Transport rate in $m^3/y/m$	Direction in °
High ADV velocity signal	Without current	18,8	158	114,2	150
	With current	18,6	159	120,3	148
Ruessink-parameterization	Without current	27,3	145	136,7	146
	With current	26,3	148	148,6	142
Isobe&Horikawa parameterization	Without current	24,5	145	111,9	146
	With current	24,0	147	121,0	142

Table 13 - mean sediment transport rates and directions

The mean transport rates in Table 13 are relatively low compared with the transport rates for high significant wave-height classes in Figure 51, because the relative frequency of waves in the high classes is low compared to the classes with wave heights between 1,5 and 3m. The transport directions for frame three are more western than the transport directions for frame 1. Bed-load sediment-transport rates from both ADV-velocity signals are more southward than the transport rates from parameterizations, in line with the findings in Figure 29. For frame 3, the calculated bed-load transport calculated with the IH-parameterized flow profile is almost the same as the transports calculated with the velocity signal. For frame 1, the IH-parameterized flow profile generates higher transport rates than the high ADV-velocity signal. This might be due to the relatively high transports from the measured velocity signal at wave class 3,5m-4m.

Weighted average for period in which at least one of the high ADV's was active		Frame 1 (-20m NAP)		Frame 3 (-16m NAP)	
		Transport rate in $m^3/y/m$	Direction in °	Transport rate in $m^3/y/m$	Direction in °
High ADV velocity signal	Without current	25,34	158	89,14	150
	With current	25,67	159	93,52	148
Ruessink-parameterization	Without current	40,17	146	105,84	147
	With current	39,02	148	115,21	142
Isobe&Horikawa parameterization	Without current	35,74	146	87,0	146
	With current	35,23	148	94,17	142

Table 14 - Weighted sediment transport rates and directions

Table 14 shows that the weighted bed-load sediment transport rates. The transport rates at frame 3 are about 50m^{3}y/m higher than those at frame 1. Both parameterizations cause higher sediment-transport rates than the measured velocity signal. For frame 3, applying currents in the calculation results in more eastern-directed sediment-transport, while for frame 1 more southward-directed sediment-transport is found. This is in line with Figure 28, which shows that the flood-tidal current at frame 3 is stronger than the flood-tidal current at frame 1.

Weighted average for year-round conditions		Frame 1 (-20m NAP)		Frame 3 (-16m NAP)	
		Transport rate in $m^3/y/m$	Direction in °	Transport rate in $m^3/y/m$	Direction in °
High ADV velocity signal	Without current	3,5	159	11,4	151
	With current	3,2	159	11,5	148
Ruessink-parameterization	Without current	4,0	143	10,8	146
	With current	3,7	145	11,8	140
Isobe&Horikawa parameterization	Without current	3,7	143	9,6	146
	With current	3,5	144	10,1	140

Table 15 - Weighted sediment transport rates and directions for year-round conditions

The weighted bed-load sediment transport rates for year-round conditions (Table 15) are about ten times as small as the transport rates during autumn 2017. In the autumn, relatively high waves occur, and episodic high waves have a large impact on the total bed-load sediment transport. The found transport rates at frame 1 are about 3,5m^3/y/m. At frame 3, the transport rates come down to 11m^3/y/m. In lower wave classes, the difference between parameterized and ADV-velocity signals is relatively low. That's why the difference in the bed-load sediment transport between the parameterizations and the ADV-velocity signals is relatively low. Weighted for year-round conditions, the IH-parameterization results in lower bed-load sediment transports than the measured velocity signal. This is an indicator that the uncertainties in weighted averaging with a small amount of measurements is high and little differences in the wave classes between 2 and 4m have a large impact on the total bed-load sediment transport rate.

7.3.6. Extrapolation for the Dutch coast

The uncertainties in the bed-load transport calculations haven't been researched yet. In a very simple straightforward calculation, it is possible to make a first estimation of the net potential sediment transport on the Dutch North-sea coast. The Dutch North-sea coastline is approximately 350 kilometres long. An onshore sediment transport rate of 3,5m^3/y/m at -20m NAP results in a total yearly onshore sediment transport of 1,2 million m^3 sand. An onshore sediment transport rate of 11m^3/y/m at -16m NAP results in a total yearly onshore sediment transport of 3,9 million m^3 sand.

The sand-nourishment policy in the 3rd coastal memorandum prescribes a yearly sand-nourishment of 12 million m^3 per year to sustain the coastal foundation, assuming no sediment transport takes place over the seaward border of the coastal foundation: -20m NAP-contour. An influx into the coastal foundation of 1,2 million m^3 is substantial compared with the yearly sand-nourishment volume.

8. Discussion

The results are influenced by the way measurements are processed to the findings. This begins with the measurements themselves. As mentioned earlier, the lowest ADV's show anomalies with respect to orbital velocities and periods, compared to the high adv's and the peak wave periods from the transformation matrix. This could be caused by turbulence due to bed roughness. Turbulences may have influenced the velocity profile from the upper ADV's as well. Also, the measurements could be influenced by objects disturbing the measured doppler effects.

In processing the data to the desired results, calculation steps had influence on the findings, the critical steps are:

- Extracting wave periods, forward and backward velocity from the data

The used WAFO-tools determine orbital wave characteristics by 'cutting' waves at their zero-upcrossings. Because the frequency of the velocity signal measurements is 16Hz, a lot of small zero-upcrossings disturbed the WAFO-tools, as displayed in Figure 22. Smoothening is applied, but smoothening with a moving average window which is too large, leads to neglecting small waves which are in de data. The mean wave periods are found on another way than peak wave periods in the transformation matrix. In this research, it is assumed that these periods are both peak wave periods.

- Averaging and weight-averaging

Data reduction by averaging is needed to reduce millions of velocity measurements to usable data. Not all data is used in some cases. The transformation matrix gives 30-minute averaged Hs data, every 3 hours. To compare the parameterizations which use the significant wave height as input with the ADV-data, all five bursts between two half hours in which the significant wave height is known are not used, although interesting values of orbital velocities could occur in those hours. When applying weighted averages, a small data set of 30-minute averaged significant wave heights remained. See Table 14.

Class	<0,5	0,5-1	1-1,5	1,5-2	2-2,5	2,5-3	3-3,5	3,5-4	4-4,5	4,5>	Total
freq frame 1	1	14	25	46	23	17	10	3	3	4	146
freq frame 3	1	7	16	21	14	12	7	5	5	3	91
Measurement campaign frame 1	1	16	32	53	28	24	14	7	6	8	189
Measurement campaign frame 3	2	18	36	50	30	20	14	7	6	6	159
2013-2017	1940	5067	3772	2153	970	392	175	63	30	46	14608

Table 16 – frequencies of wave heights in different wave height classes

The frequencies for the entire measurement campaign are the frequencies of the Hs-values in which at least one of the high ADV's of both measurement frames collect data. All classes with 5 of fewer measurements are marked orange. Weighted averaging with classes with only 5 or fewer measurements cause large uncertainties for the final results, especially when these classes contain

the measurements with the highest impact on the bed-load sediment transport, containing significant wave heights higher than 3,5m.
Another remark with weight-averaging, is that wave-averaging groups sediment transports, partly influenced by currents in wave-height groups, while currents and wave-heights are not correlated.

- Simplification

Some processes are simplified in this research. The Van Rijn (2007) bed-load transport formulations act like a model in a certain way, because they predict ripples and megaripples and calculate bed-shear stresses with these predicted (mega)ripples, instead of using data. Furthermore, in this research, the heights of the ADV-sensors relative to the bed are kept constant. These heights are likely to change over time due to changing bedforms. The water depths are kept constant as well at 16m and 20m, while water levels rise and fall during a tidal cycle. The sensitivity analysis shows that water height has a substantial effect on bed-load sediment transport. The largest simplification is using the currents measured with the upper ADV's (0,5m above bed) as depth-averaged currents. The depth-averaged currents are expected to be higher than the currents at 0,5m above bed.

Another simplification is the choice for the type of period used. The extracted wave periods from the ADV-measured velocity signals with the WAFO-tools is directly used as input in the Van Rijn (2007) formulations, whereas the peak wave period is needed. Determining the peak wave period could be done using spectral analysis, which is not done in this research. This will certainly have influence on the results.

9. Conclusion and recommendations

Per sub-question, the found answers in the results of this research are described below. After answering the sub-questions, recommendations on ….? Are made.

6. *What are the near-bed wave characteristics measured on different locations on the lower shoreface?*
    a. *Wave orbital velocity magnitude*
    b. *Wave orbital velocity skewness and asymmetry*

On two locations near the Ameland Inlet at 20 and 16 meter water depth, the mean weighted measured significant forward orbital velocities during autumn 2017 are 0,37m/s and 0,50m/s respectively. At high energetic events, waves with a significant wave height above 4m occur. During these events, significant forward orbital velocities up to 0,9m/s and 1,5m/s are measured at -16m NAP and -20m NAP respectively.

The observed wave skewnesses are relatively low, compared to the skewnesses found by Ruessink et al. (2012) with smaller water depth conditions. The mean weighted measured Su-skewness is 0,04 for frame 1 and 0,06 for frame 3. During episodes with wave heights of about 4m, Su-skewnesses of 0,25 and 0,10 for Frames 3 and 1 respectively are observed. Only for waves higher than 3 meter, waves at 16m water depth are substantially more skewed than waves at 20m water depth. For lower waves, the skewness is too small to make conclusions about the impact of water depth on skewness. Negative skewness does occur at both water depths during low-wave events. Negative skewnesses were also observed by Ruessink et al. with smaller water depth conditions. On both locations, the measured asymmetry profile was spiked, but the average asymmetry is negligible.

7. *How do measured orbital velocities, skewness and asymmetry on the lower shoreface compare to calculated orbital velocities by the parameterization proposed by Isobe & Horikawa (1982) and the parameterization by Ruessink et al (2012)?*

The Ruessink-parameterization shows higher forward significant orbital velocities than the Isobe-Horikawa parameterization. Both parameterizations represent the forward significant velocity well, the difference in velocity between both parameterizations is in most cases smaller than the difference between the velocity of the parameterized velocity profiles and the measured velocities.

Whereas the measured velocity signal show negative skewnesses, the parameterizations only generate positively skewed wave profiles. At higher waves, the Ruessink-parameterization starts to underestimate the wave skewness. The Isobe&Horikawa parameterization approximates the skewness using the Su-indicator the best. The Ru-parameterization might not show reliable results for the measured velocity profile, due to the used method to find the peak velocities.

The Ruessink-parameterized wave profiles show completely symmetric waves. This is in line with the measured asymmetries. The parameterization by Isobe&Horikawa is unable to show asymmetry.

8. *What is the influence of water depth on bed-load sediment transport on the lower shoreface due to orbital wave motion?*

The influence of the parameter 'water depth' on bed-load sediment transport in Van Rijn (2007) bed-load formulations is large at small water depths (<10m NAP). With used parameter settings for significant wave height, peak wave period , significant grain size and current, water depth causes a decrease of about two third of the 600m^3/y/m bed-load sediment transport at -15m, between -15m NAP and -20m NAP.

9. *What is the influence of grain size of sediment on sediment movement on the lower shoreface due to orbital wave motion?*

Using the minimum and maximum found grain size values near the study area as range, the difference in bed-load sediment transport is relatively small, at both water depths in which the influence is investigated, -20m and -16m NAP. The increase in bed-load sediment transport does not exceed 10% of the mean bed-load transport.

10. *What is the potential bed-load sediment transport on the Dutch lower shoreface due to orbital wave* motion?
    a. Using the flow velocities from the Isobe & Horikawa and Ruessink parameterizations;
    b. Using the measured flow velocities?

The potential bed-load sediment transport at the measurement locations on the lower shoreface near the Amelander Zeegat using the Isobe & Horikawa and Ruessink parameterizations, weighted for year-round conditions comes down to 3,7m^3/y/m and 3,5m^3/y/m respectively for -20m NAP and 11,8m^3/y/m and 10,1m^3/y/m at -16m NAP, in South-East direction. The direction and magnitude are mainly influenced by waves at both water depths.

The potential bed-load sediment transport at the measurement locations on the lower shoreface near the Amelander Zeegat using the measured velocity signals, weighted-averaged for year-round conditions comes down to 3,2m^3/y/m for -20m NAP and 11,5m^3/y/m at -16m NAP, in South by South-East direction. The direction and magnitude are mainly influenced by waves.
Using the parameterizations as input for the Van Rijn (2007) formulations causes overestimation of the wave-related transport component, as the parameterizations overestimate the orbital velocities. The Isobe&Horikawa parameterization approximates the bed-load transport rate found with the measured velocity profile best.

On the measurement locations near the Amelander Zeegat, the difference in transport directions of about 5^o could be caused by differences in near-bed orbital wave directions and water surface wave directions, due to bathymetric effects.

Because the influence of orbital wave velocity and direction on sediment transports is large compared to other parameters, it is possible to assume that the magnitude of bed-load sediment transport on other locations on the Dutch lower shoreface on -20m and -16m NAP is more or less the same as the observed orbital velocities near the Amelander Zeegat. An estimation of the total yearly sediment-transport rate for the Dutch coast is about 1 Mm^3/year at -20m NAP and nearly 4Mm^3/year for -16m NAP.

Recommendations
For further research, a few recommendations could be provided. First, a quantification of the uncertainties in the presented research is needed. Other research into the subject of bed-load sediment transport on the Dutch lower shoreface, by Van de Meene and Van Rijn (2000) shows uncertainties larger than the found sediment transport rates itself for example. To base policy advises on this research, the range of uncertainties is crucial to know.

Also, an extra look at the Van Rijn (2007) transport formulations is useful. The formulations determine bed-load transport by integrating the bed-load transport over a parameterized waveshape. This waveshape is the waveshape proposed by Isobe & Horikawa. It is interesting to look at the differences in sediment transport when applying the Ruessink-waveshape, because the Ruessink-waveshape has the possibility to show asymmetry, so the effects of asymmetry on bed-load transport could be determined. It is also possible to implementing a raw velocity signal from the ADV-data.

None of the two parameterizations shows negative skewness. Research into developing a new parameterization which could show negative skewness could be done, to approximate the natural conditions better than currently used parameterizations.

To find a better insight in cross-shore sediment transports on the Dutch lower shoreface, data from other measurement frames on other positions on the Dutch shoreface could be used to validate the data found at the lower shoreface near the Amelander Zeegat. This makes the findings from this research more robust. More data at different depths could be used to make a cross-shore profile with sediment transports at different depths. This research found potential bed-load sediment transport at -20m and -16m NAP, but extra information at other depts could provide enough data to interpolate sediment transport over different depths.

Figure 28 shows a difference in wave direction between both measurement frames, and a different pattern in tidal current, that could be caused by bathymetric effects. Further research could determine what the effects of the bathymetry on tidal current and wave patterns is near the Amelander Zeegat.

The last recommendation is to expand this research with other sensors attached to the used measurement frames: The Acoustic Doppler current profiler (ADCP) and 3D Sand Ripple Profiling Logging Sonar (3DSRPLS). With the ADCP, currents at different water depths above the sensor could be measured, from which the depth-averaged velocity profile needed for the Van Rijn (2007) formulations could be calculated. The 3DSRPLS could measure the developments in the seabed. With this sensor, the calculated bed-load sediment transports could be validated.

10. References

Abreu, T. A. (2011). *de Azevedo Abreu, Tiago André Martins. Coastal sediment dynamics under asymmetric waves and currents: measurements and simulations.* Coimbra, Portugal: Universidade de Coimbra.

Abreu, T., Silva, P., Sancho, F., & Temperville, A. (2010). Analytical approximate wave form for asymmetric waves. *Coastal Engineering*, 656-667.

Albernaz, M. B., Ruessink, B., Walstra, D., Jagers, H., Tonnon, P., Grasmeijer, P., & Kleinhans, M. (2018). Parameterization of wave orbital motion and its effect on long term morphological development in the nearshore.

Browning, J., Miller, K., McLaughin, P., Kominz, M., Sugarman, P., Monteverde, D., . . . Hernández, J. (2006). Quantification of the effects of eustasy, subidence, and sediment on Miocene sequences, mid-Atlantic margin of the United States. *GSA bulletin*, 567-588.

De Ronde, J. (2008). *Toekomstige langjarige suppletiebehoefte.* Delft.

Fockert, A. d., & Luijendijk, A. (2011). *Wave look-up table Building with Nature.* Delft.

Goring, D. G., & Nikora, V. I. (2002). Despiking Acoustic Doppler Velocimeter Data. *Journal of Hydraulic Engineering*, 117-126.

Isobe, M., & Horikawa, K. (1982). Study on water particle velocities of shoaling and breaking waves. *Coastal Engineering in Japan*, 109-123.

Malarkey, J., & Davies, A. (2012). Free-stream velocity descriptions under waves with skewness and asymmetry. *Coastal Engineering*, 78-95.

Ministry of Infrastructure and Water Management. (2017). *Coastal Genesis 2.0 - Knowledge for a safe coast.* Ministry of Infrastructure and Water Management, National Water and Climate Knowledge and Innovation Programme.

Mol, J. (2018). *KG2 DVA metadata frame 3.* RWS CIV.

Mulder, J. (2000). *Zandverliezen in het Nederlandse kustsysteem - Advies voor Dynamische Handhaven in de 21e eeuw.* Rijksinstituut voor Kust en Zee.

Nortek AS. (2005). *Vector current meter user manual.*

Rijkswaterstaat. (2018, June 12). *Getij*. Retrieved from Rijkswaterstaat: https://www.rijkswaterstaat.nl/water/waterdata-en-waterberichtgeving/waterdata/getij/index.aspx

Ruessink, B., Ramaekers, G., & Van Rijn, L. (2012). on the parameterization of the free-stream non-linear wave orbital motion in nearshore morphodynamic models. *Coasta Engineering*, 56-63.

The WAFO group. (2017). *WAFO - a Matlab Toolbox for Analysis of Random Waves and Loads - Tutorial for WAFO version 2017.* Lund: Lund University.

Van de Meene, J., & Van Rijn, L. (2000). The shoreface-connected ridges along the central Dutch coast - part 1: field observations. *Continental shelf research*, 2295-2323.

Van der Werf, J., Grasmeijer, B., Hendriks, E., Van der Spek, A., & Vermaas, T. (2017). *Literature study Dutch lower shoreface.* Delft: Deltares.

Van Rijn, L. (1993). *Principles of sediment transport in rivers, estuaries, and coastal seas.* Oldemarkt: Aqua Publications.

Van Rijn, L. (2007). Unified View of Sediment Transport by Currents and waves. I: Initiation of Motion, Bed Roughness, and Bed-Load Transport. *Journal of Hydraulic Engineering*, 649-667.

Van Rijn, L. (2013). *Principles of fluid flows and surface waves in rivers, estuaries, seas and oceans.* Oldemarkt: Aqua publications.

Van Rijn, L., & Walstra, D. (2004). *Description of TRANSPOR2004 and Implementation in Delft3D-ONLINE.*

VROM, M. v. (2004). *Nota Ruimte.* Den Haag.

Appendix A – Mathematic representation of parameterizations

Isobe & Horikawa (1982)

$$\hat{U}_{w,for} = \hat{U}_{w,max}[0.5 + (r_{max} - 0.5)\tanh(\frac{r_a - 0.5}{r_{max} - 0.5})]$$
$$\hat{U}_{w,back} = \hat{U}_{w,max} - \hat{U}_{w,for}$$
$$\hat{U}_{w,max} = 2\,r\,\hat{U}_w$$

With:

$$r = -0.4\frac{H_s}{h} + 1$$
$$A_1 = -0.0049(T_1)^2 - 0.069T_1 + 0.2911$$
$$r_a = -5.25 - 6.1\tanh(A_1U_1 - 1.76)\,;\, r_a = 0.5 \text{ if } r_a < 0.5$$
$$r_{max} = -2.5\frac{h}{l} + 0.85;\, r_{max} = 0.75 \text{ if } r_{max} > 0.75 \text{ and } r_{max} = 0.62 \text{ if } r_{max} < 0.62$$
$$U_1 = \frac{\hat{U}_{w,max}}{\sqrt{gh}}$$
$$\hat{U}_w = \frac{\pi H_s}{T_p\sinh(kh)}$$

$\hat{U}_w$	peak orbital velocity near bed based on linear theory (with H_s and T_p) (m/s)
H_s	significant wave height (m)
L	wave length (m)
T_p	peak wave period (s)
h	water depth
k	Wave number
A, r_a, r_{max}	Parameters

Waveshape:

$$U_{w,for} = \hat{U}_{w,for}\sin(\frac{2\pi t}{2T_{for}})$$

For $0<t<T_{on}$

$$U_{w,back} = -\hat{U}_{w,back}\sin(\frac{2\pi(t - T_{for})}{2T_{back}})$$

For $T_{for}<t<T_{back}$

$$T = T_{for} + T_{back}$$

$$T_{for} = \frac{\hat{U}_{w,back}\,T}{\hat{U}_{w,for} + \hat{U}_{w,back}}$$
$$T_{back} = \frac{\hat{U}_{w,for}\,T}{\hat{U}_{w,for} + \hat{U}_{w,back}}$$

T	wave period (s)
T_{for}	duration of forward phase (s)
T_{back}	duration of backward phase (s)

Ruessink

$$U_t = \hat{U}_w\sqrt{1 - r^2}\,\frac{\sin(\omega t) + \dfrac{r}{t - \sqrt{1 - r^2}}\sin\varphi}{1 - r\cos(\omega t + \varphi)}$$

U_t = horizontal velocity (m/s)

r= wave form coefficient
φ=phase angle
$\hat{U}_w = 0.5|\hat{U}_{for}| + |\hat{U}_{back}|$
r varies in range -1<1
φ varies in the range -90°<φ<90°

$$UR = \frac{3\, H_s\, k}{8(kh)^3}$$

UR=Ursell number
H_s= significant wave height (m)
h=water depth (m)
k=wave number (m)

$$r = \tanh(0.9305 \frac{0.8507}{1 + e^{-1.586 - 3.367 \log(UR)}})$$

$$\varphi = -90^o \tanh(\frac{0.815}{UR^{0.672}})$$

With

$$\hat{U}_w = \frac{\pi H_s}{T_p \sin(kh)}$$

In which T_p is peak wave period (s)